Nanosecond Molecular Dynamics Simulations of Parallel and Antiparallel Guanine Quadruplex DNA Molecules

Nad'a Špačková,[†,‡,§] Imre Berger,[||] and Jiří Šponer*[,‡]

Contribution from the Institute of Biophysics, Academy of Sciences of the Czech Republic, Královopolská 135, 612 65 Brno, Czech Republic, J. Heyrovský Institute of Physical Chemistry, Academy of Sciences of the Czech Republic, Dolejškova 3, 182 23 Prague, Czech Republic, Department of Physical Electronics, Faculty of Science, Masaryk University, Kotlářská 2, 611 37 Brno, Czech Republic, and Institute for Molecular Biology and Biophysics, ETH-Hönggerberg, CH-8093 Zürich, Switzerland

Received December 28, 1998. Revised Manuscript Received March 29, 1999

Abstract: Molecular dynamics (MD) simulations are presented of four-stranded G-DNA molecules formed by the sequences $d(G_4)$ and $d(G_4T_4G_4)$. Starting coordinates are based on high-resolution X-ray structures or NMR data. Simulations of the all-parallel $d(G_4)$ quadruplex with sodium cations in the central ion channel yield exceptionally stable trajectories on the nanosecond scale. Simulations without cations in the channel show destabilization of the G-DNA structure, underscoring the central role of these ions for the structural integrity of the molecule. Further simulations reveal that the cation-stabilized $d(G)_4$ stem can adopt an alternative very stable conformation involving a guanine base triad. Simulations of $d(G_4T_4G_4)$ quadruplexes indicate a similar rigidity and stability of the antiparallel guanine stem as for the parallel $d(G_4)$ conformer. The simulations further demonstrate significant geometrical plasticity of the thymine residues arranged in four-nucleotide loops, including loop geometries capable of coordinating to a sodium cation from the ion channel via thymine carbonyl groups. All simulations were carried out with the AMBER4.1 force field, using the particle mesh Ewald (PME) technique for electrostatic interactions, with the total length of all simulations reaching 25 ns. The calculations indicate some inaccuracies of the force field description for a direct interaction between cations and guanine quartets likely due to the pair-additive nature of the force field. Moderate perturbation of the hydrogen bonding geometries in quartet layers is noted, giving rise to bifurcated hydrogen bonds. However, the overall results of the simulations show an excellent performance of the PME MD technique and AMBER4.1 force field for these unusual nucleic acids.

Introduction

Deoxynucleic acid molecules can adopt many different shapes. Besides the established A, B, and Z duplex forms, DNA can form triplexes and also structures such as four-stranded intercalated cytosine-rich i-DNA and the G-DNA quadruplex formed by guanine-rich DNA (Figure 1). DNA sequences with stretches of guanine residues are present in the genome of cells, in gene regulatory regions, and also in centromeric and telomeric DNAs among others.[1] Telomeric DNA consists of concatamers of tandemly arranged short guanine-rich DNA sequence motifs and characteristically possesses a 3′ terminal overhang of several guanine-rich repeats.[1a−c] The unusual properties associated with these overhangs[2] led to the proposal that they can form four-stranded conformations involving guanine quadruplex stems.[3]

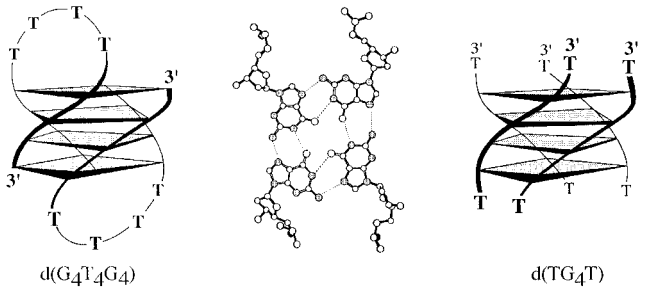

Figure 1. Four-stranded G-DNA molecules. Schematic drawing of an antiparallel guanine quadruplex (left) formed by *Oxytricha* telomeric DNA $d(G_4T_4G_4)$.[4a] The thymine residues are arranged in four-nucleotide loops. This quadruplex is stabilized by guanine quartet layers (center) with alternating syn−anti glycosidic bond conformations (nitrogen atoms are shaded). The parallel guanine quadruplex (right) formed by $d(TG_4T)$ has all guanines anti.[4c−e] 3′ Termini are marked.

† Institute of Biophysics, Academy of Sciences of the Czech Republic.
‡ J. Heyrovský Institute of Physical Chemistry, Academy of Sciences of the Czech Republic.
§ Masaryk University.
|| ETH-Hönggerberg.
* To whom correspondence should be addressed at the Institute of Physical Chemistry, Prague. E-mail: sponer@indy.jh-inst.cas.cz.

(1) (a) Moyzis, R. K.; Buckingham, J. M.; Cram, L. S.; Dani, M.; Deaven, L. L.; Johns, M. D.; Meyne, J.; Ratliff, R. L.; Wu, J. R. *Proc. Natl. Acad. Sci. U.S.A.* **1988**, *85*, 6622−6626. (b) Henderson, E. R.; Hardin, C. C.; Walk, S. K.; Tinoco, I.; Blackburn, E. *Cell* **1987**, *51*, 899−908. (c) Klobutcher, L. A.; Swanton, M. T.; Donini, P.; Prescott, D. M. *Proc. Natl. Acad. Sci. U.S.A.* **1986**, *78*, 3015−3019. (d) Sundquist, W. I.; Heaphy, S. 1993, *Proc. Natl. Acad. Sci. U.S.A.* **1993**, *90*, 3393−3397. (e) Murchie, A. I., Lilley, D. M. J. *Nucleic Acids Res*. **1992**, *20*, 49−53. (f) Akman, S. A., Lingeman, R. G., Doroshow, J. H., Smith, S. S. *Biochemistry* **1991**, *30*, 8648−8653.

(2) (a) Cech, T. R. *Nature* **1988**, *332*, 777−778. (b) Lipps, H. J.; Gruissem, W.; Prescott, D. M. *Proc. Natl. Acad. Sci. U.S.A.* **1982**, *79*, 2495−2499. (c) Oka, Y.; Thomas, C. A. *Nucleic Acids Res.* **1987**, *15*, 8877−8898.

(3) (a) Williamson, J. R.; Raghuram, M. K., Cech, T. R. *Cell* **1989**, *59*, 871−880. (b) Sundquist, W. I.; Klug, A. *Nature* **1989**, *342*, 825−829. (c) Sen, D.; Gilbert, W. *Nature* **1988**, *334*, 364−366.

10.1021/ja984449s CCC: $18.00
Published on Web 05/27/1999

Structural studies on guanine-rich DNA sequences revealed many details of this quadruplex motif at high resolution.[4]

The structure and dynamic behavior of nucleic acid molecules is a primary target of theoretical analyses, and several molecular modeling studies on quadruplex structures have been published in the past.[5] In recent years, however, significant qualitative improvement has been achieved in this field. In particular, the introduction of the particle mesh Ewald (PME) technique for long-range electrostatic interactions[6] proved to be essential toward obtaining stable trajectories in molecular dynamics (MD) simulations of solvated nucleic acid molecules on up to the nanosecond time scale.[7] Improvement was further achieved in the parametrization of the force fields,[8] although their reliability is still somewhat limited by approximations such as atom−atom pair additivity, conformation-independent atomic charges, and others.[9] High-level ab initio calculations allowed refinement and verification of the force fields.[8,9b,10] Nanosecond MD simulations provided numerous interesting results while also illustrating some of the current limitations of the technique.[11]

Recently, we reported a nanosecond MD study of a four-stranded intercalated cytosine-rich i-DNA, d(C_4).[12] This study was based on a total of 15 ns of simulations and underscored the unusual conformational rigidity of this intercalated quadruplex DNA motif.[13] The analysis indicated that the inclusion of backbone interactions and hydration effects sufficed to balance the rather large electrostatic repulsion[14] of consecutive closely spaced (3.1 Å) hemiprotonated cytosine·cytosine$^+$ (C·C$^+$) base pairs in the i-DNA structure. The stable arrangement in i-DNA of consecutive C·C$^+$ base pairs, each carrying a positive charge, contrasts with a study on protonated triplexes where consecutive protonated cytosine residues involved in CG·C$^+$ base triplets effectively destabilize the structure.[15] Here, the results of MD simulations on one hand and experimental studies on the other were found to be in excellent agreement.

In the present study, we report a set of unconstrained MD simulations of the guanine-rich counterpart of i-DNA, namely the G-DNA quadruplex. The total length of all simulations reached 25 ns (see Table 1). One guanine-rich structure investigated here is formed by four strands with the sequence d(TG_4T) that are arranged in an all-parallel fashion in a quadruplex array stabilized by quartets of cyclically hydrogen bonded guanine residues with all glycosidic bonds in anti conformation.[4c−e] The focus of our analysis was the guanine stem of this molecule built by four adjacent guanine quartets. As high-resolution X-ray diffraction studies revealed, a vertical alignment of consecutive positive charges exists along the helical axis of this molecule due to a string of monovalent sodium cations located in the channel between the guanine residues forming the quartet layers.[4c] In this respect, there is a similarity between this G-DNA quadruplex and i-DNA, where the charge alignment in the molecule center stems from the hemiprotonation of the cytosine base pairs.[12,13] Our studies show that the all-parallel guanine quadruplex stem including the monovalent cations in the central channel is rigid and very stable on a nanosecond scale, with exceptionally close agreement to the high-resolution crystal coordinates[4c,d] used as a starting model. The mobility of cations in G-DNA quadruplex structures is discussed, and the performance of the force field to describe guanine−cation interactions is compared to that of quantum chemical calculations. Further, we demonstrate the essential role of the cations in stabilizing this structure, as simulations with the cations removed from the central channel lead to drastic rearrangements in the molecule including temporary formation of triads of guanine residues. However, we show that the "triad" structure with one slipped strand is stabilized upon incorporation of cations into its channel and shows (on the nanosecond scale) the same stability as the native stem. It represents an alternative conformational substate to the native stem with a lifetime much above the nanosecond scale. Finally, we compare the behavior of antiparallel guanine quadruplexes formed by sequences present in telomeric DNA to those of the all-parallel structure in MD simulations.

(4) (a) Kang, C. H.; Zhang, X.; Ratliff, R.; Moyzis, R.; Rich, A. *Nature* **1992**, *356*, 126−131. (b) Smith, F. W.; Feigon, J. *Nature* **1992**, *356*, 164−168. (c) Laughlan, G.; Murchie, A. I. H.; Norman, D. G.; Moore, M. H.; Moody, P. C. E.; Lilley, D. M. J.; Luisi, B. *Science* **1994**, *265*, 520−524. (d) Phillips, K.; Dauter, Z.; Murchie, A. I. H.; Lilley, D. M. J.; Luisi, B. *J. Mol. Biol.* **1997**, *273*, 171−182. (e) Phillips, K.; Luisi, B. *Science* **1998**, *281*, 883. (f) Smith, F. W.; Schultze, P.; Feigon, J. *Structure* **1995**, *3*, 997−1008. (f) Kettani, A.; Kumar, R. A.; Patel, D. J. *J. Mol. Biol.* **1995**, *254*, 638−656. (g) Aboud-ela, F.; Murchie, A. I. H.; Norman, D. G.; Lilley, D. M. J. **1994**, *243*, 458−471. (h) Bouaziz, S.; Kettani, A.; Patel, D. J. *J. Mol. Biol.* **1998**, *282*, 637−652. (i) Schultze, P.; Smith, F. W.; Feigon, J. *Curr. Biol.* **1994**, *2*, 221−223.

(5) (a) Hardin, C. C.; Ross, W. S. *J. Am. Chem. Soc.* **1994**, *116*, 6080. (b) Mohanty, D.; Bansal, M. *Biophys. J.* **1995**, *69*, 1046−1067. (c) Tohl, J.; Eimer, W. *Biophys. Chem.* **1997**, *67*, 177−186. (d) Strahan, G. D.; Keniry, M. A.; Shafer, R. H. *Biophys. J.* 1998, *75*, 968−974. (e) Mohanty, D.; Bansal, M. *Biopolymers* **1994**, *34*, 1187−1211. (f) Strahan, G. D.; Shafer, R. H.; Keniry, M. A. *Nucleic Acids Res.* **1994**, *22*, 5447−5455. (g) Balagurumoorthy, P.; Brahmachari, S. K.; Mohanty, D.; Bansal, M.; Sasisekharan, V. *Nucleic Acids Res.* **1992**, *20*, 4061−4067.

(6) (a) York, D. M.; Darden, T.; Pedersen, L. G. *J. Chem. Phys.* **1993**, *99*, 8345−8348. (b) York, D. M.; Yang, W.; Lee, H.; Darden, T.; Pedersen, L. G. *J. Am. Chem. Soc.* **1995**, *117*, 5001−5002.

(7) Lee, H.; Darden, T.; Pedersen, L. *Chem. Phys. Let.* **1995**, *243*, 229−234. (b) Cheatham, T. E., III; Miller, J. L.; Fox, T. Darden, T. A.; Kollman, P. A *J. Am. Chem. Soc.* **1995**, *117*, 4193−4194.

(8) Cornell, W. D.; Cieplak, P.; Bayly, C. I.; Gould, I. R.; Merz, K. M.; Ferguson, D. M., Jr.; Spellmeyer, D. C.; Fox, T.; Caldwell, J. W.; Kollman, P. A. *J. Am. Chem. Soc.* **1995**, *117*, 5179−519.

(9) (a) Šponer, J.; Gabb, H. A.; Leszczynski, J.; Hobza, P. *Biophys. J.* **1997**, *73*, 76−87. (b) Halgren, T. A. *Curr. Opin. Struct. Biol.* **1995**, *5*, 205−210 and references therein.

(10) Hobza, P.; Kabeláč, M.; Šponer, J.; Mejzlík, P.; Vondrášek, J. *J. Comput. Chem.* **1997**, *18*, 1136−1150.

(11) (a) Weerasinghe, S.; Smith, P. E.; Pettitt, B. M. *Biochemistry* **1995**, *34*, 16269−16278. (b) Cheatham, T. E., III; Kollman, P. A. *J. Mol. Biol.* **1996**, *259*, 434−444. (c) Shields, G. C.; Laughton, C. A.; Orozco, M. *J. Am. Chem. Soc.* **1997**, *119*, 1463−1469. (d) Young, M. A.; Jayram, B.; Beveridge, D. L. *J. Am. Chem. Soc.* **1997**, *119*, 59−69. (e) Louise-May, S.; Auffinger, P.; Westhof, E. *Curr. Opin. Struct. Biol.* **1996**, *6*, 289−298. (f) Feig, M.; Pettitt, B. M. *J. Phys. Chem. B* **1997**, *101*, 7361−7363. (g) Shields, G. C.; Laughton, C. A.; Orozco, M. *J. Am. Chem. Soc.* **1998**, *120*, 5895−5904. (h) Auffinger, P.; Westhof, E. *Curr. Opin. Struct. Biol.* **1998**, *8*, 227−232 (i) Feig, M.; Pettitt, B. M. *Biophys.* J. **1998**, *7*, *5* 134−149. (j) Young, M. A.; Beveridge, D. L. *J. Mol. Biol.* **1998**, *281*, 675−687. (k) Srinivasan, J.; Cheatham, T. E., III; Cieplak, P.; Kollman, P. A.; Case, D. A. *J. Am. Chem. Soc.* **1998**, *120*, 9401−9409. (l) Cheatham, T. E., III; Srinivasan, J.; Case, D. A.; Kollman, P. A. *J. Biomol. Struct. Dyn.* **1998**, *16*, 265−280. (m) Simmerling, C.; Fox, T.; Kollman, P. A. *J. Am. Chem. Soc.* **1998**, *120*, 5771−5782. (n) Cheatham, T. E., III; Brooks, B. R. *Theor. Chem. Acc.* **1998**, *99*, 279−288. (o) Cheatham, T. E., III; Kollman, P. A. In *J. Structure, Motion, Interaction and Expression of Biological Macromolecules*; Sarma, R. H., Sarma, M. H., Eds.; Adenine Press: Guilderland, NY, 1998; pp 99−116. (p) Souza, O. N.; Ornstein, R. L. *J. Biomol. Struct. Dyn.* **1997**, *14*, 607−611. (q) Cheatham, T. E., III; Cieplak, P.; Kollman, P. A. *J. Biomol. Struct. Dyn.* **1999**, *16*, 845−862.

(12) Špačková, N.; Berger, I.; Egli, M.; Šponer, J. *J. Am. Chem. Soc.* **1998**, *120*, 6147−6151.

(13) (a) Gehring, K.; Leroy, J.-J.; Gueron, M. *Nature* **1993**, *363*, 561−565. (b) Nonin, S.; Leroy, J.-L. *J. Mol. Biol.* **1996**, *261*, 399−414. (c) Leroy, J.-L.; Gueron, M. *Structure* **1995**, *3*, 101−120. (d) Chen, L.; Cai, L.; Zhang, X.; Rich, A. *Biochemistry* **1994**, *33*, 13540−13545. (e) Kang, C.; Berger, I.; Lockshin, C.; Ratliff, R.; Moyzis, R.; Rich, A. *Proc. Natl. Acad. Sci. U.S.A.* **1994**, *91*, 11636−11640. (f) Berger, I.; Kang, C.; Fredian, A., Ratliff, R.; Moyzis, R.; Rich, A. *Nat. Struct. Biol.* **1995**, *2*, 416−425. (g) Berger, I.; Egli, M.; Rich, A. *Proc. Natl. Acad. Sci. U.S.A.* **1996**, *93*, 12116−12121. (h) Gallego, J.; Golden, E. B.; Stanley, D. E.; Reid, B. R. *J. Mol. Biol.* **1999**, *285*, 1039−1052.

(14) Šponer, J.; Leszczynski, J.; Vetterl, V. Hobza, P. *J. Biomol. Struct. Dyn.* **1996**, *13*, 695−707.

(15) Soliva, R.; Laughton, C.; Luque, F. J.; Orozco, M. *J. Am. Chem. Soc.* **1998**, *120*, 11226−11233.

Table 1. Summary of Simulations Carried Out in This Study

starting structure	cations in channel	main purpose of the simulation	length[a] (ns)
1, crystal structure[b]	three Na^+	basic investigation of the parallel stem	3.4[c]
2, crystal structure[b]	two Na^+	role of the cations in structure and stability	2.7
3, crystal structure[b]	no ions	role of the cations in structure and stability	3.4[d]
4, crystal structure[b]	three smaller Na^+	test of cation mobility and force field	2.0
5, snapshot from simul. 3[e]	two Na^+	stabilization of the "slipped" structure	3.0
6, final str. from simul. 5[e]	three Na^+	further investigation of the "slipped" structure	2.0
7, crystal structure[f]	three Na^+	basic investigation of the X-ray antip. structure	2.5
8, crystal structure[f]	three K^+	an independent simulation to 7, test of K^+ vs Na^+	2.5
9, NMR structure[g]	three Na^+	investigation of diagonally looped structure	3.5

[a] Production simulation. [b] Parallel quadruplex d(TG_4T), X-ray, Phillips et al.[4c,d] [c] Including 0.8 ns at elevated temperature of 400 K. [d] Including 1.1 ns at elevated temperature of 400 K. [e] Simulation of parallel G-stem with a "slipped" strand. [f] Antiparallel edge-looped quadruplex d($G_4T_4G_4$)$_2$, X-ray, Kang et al.[4a] [g] Antiparallel diagonal-looped quadruplex d($G_4T_4G_4$)$_2$, NMR, Schultze and Feigon.[4b]

Methods

Molecular Dynamics Simulations. All calculations were carried out using the AMBER4.1[16] program with a Cornell et al.[8] force field. The nucleic acid molecules were surrounded by a periodic box of water molecules described by the TIP3P potential.[17] The periodic box was extended to a distance of 10 Å from any solute atom. The number of explicit water molecules included in the simulations varied from 2600 to 4900, depending on the solute molecule. The molecules were neutralized by Na^+ or K^+ cations using standard parameters for the Cornell et al. force field[8] (we used van der Waals radii of 1.868 Å for Na^+ and 2.658 Å for K^+, and the corresponding well depths were 0.002 77 and 0.000 328 kcal/mol[5a]). We point out that the force field is pair additive; this is important for a proper understanding of the limitations in the description of the cation−solute interactions discussed below. Internal cations were added into the channel either using crystallographic data for the high-resolution parallel G-DNA structure by Luisi et al.[4d] or manually into cavities between G-quartets in all other cases. The other cations were initially placed into the most negative locations using Coulombic potential terms with the LEAP[16] module of AMBER4.1 (except a simulation without ions in the channel where all ions were added at equidistance from phosphate oxygen atoms spaced 3.5 Å from the phosphorus atom using the EDIT[16] module of AMBER4.1). All cations were considered as part of the solvent including those in the channel. Calculations were carried out using the Sander module of AMBER 4.1 with SHAKE on the hydrogen atoms with a tolerance of 0.0005 Å and a 2 fs time step. A 9 Å cutoff was applied to Lennard-Jones interactions. Simulations were performed using the Berendsen temperature coupling algorithm (with a time constant of 0.2 ps). The nonbonded pair list was updated every 10 steps. Equilibration was started by 1000 steps of minimization with the positions of the nucleic acid fixed. After this initial equilibration, all subsequent simulations were performed using the particle mesh Ewald method (PME) for inclusion of long-range electrostatic interactions into calculations without truncation. The PME charge grid spacing was approximately 1.0 Å, and the charge grid was interpolated using a cubic B-spline with the direct sum tolerance of 10^{-6} at the 9 Å direct space cutoff. To speed up the fast Fourier transform in the calculation of the reciprocal sum, the size of the PME charge grid was chosen to be a product of powers of 2, 3, and 5. For dynamics runs after minimizations, initial velocities were assigned from a Maxwellian distribution. Equilibration was continued by 25 ps of PME dynamics, with the position of the nucleic acid fixed. Subsequently, 1000 steps of minimization were carried out with 25 kcal/(mol Å^2) restraints placed on all solvent atoms, continued by 3 ps of MD simulation using the same restraint. This equilibration was followed by five rounds of 1000-step minimization with solute restraints reduced by 5 kcal/(mol Å^2) in the course of each round. Then 20 ps of MD followed, with the system heated from 100 to 300 K over 2 ps. Equilibration was continued by several nanoseconds of production simulation. Coordinates were written to trajectory files after each picosecond.

It is well-established that the incomplete energy conservation and the weak-coupling method to control temperature can induce energy drain. Scaling of the temperature occurred by scaling the velocity, and it could lead to a growth of the center of mass translational motion (cold solute/hot solvent problem).[18] To minimize this problem, the center of mass velocity was removed during the production dynamics periodically in intervals of 10 ps.

The results were analyzed using the Carnal module of AMBER 4.1. No extra processing of the averaged structures obtained by the Carnal module was performed. Solvent and counterion distributions were monitored by binding atom positions from rms coordinate fit frames over all DNA atoms at 1-ps intervals into (0.5 Å)^3 grids over 1-ns portions of the trajectories,[19] with the aid of program USCF MidasPlus.[19b]

Several production runs were extended by a simulation at an elevated temperature of 400 K. A similar protocol of heating was used as for the equilibration, lasting for 20 ps (i.e., the process was slower than for the equilibration).

Table 1 summarizes all simulations that have been carried out in the course of this study. The same standard equilibration protocol was applied to all simulations including 4 and 5, where additional cations were moved into the channel of a structure taken from one of the preceding simulations.

Ab Initio Calculations of Guanine−Cation Complexes. The structures of guanine·Na^+ and guanine·Li^+ complexes were optimized within the Hartree−Fock approximation utilizing the 6-311+G(d,p) basis set of atomic orbitals, while the M−O6−C6 angle (M: ion) was kept frozen at a value of 135°. This type of constrained geometry maintains the position of the cation with respect to guanine assuming an in-plane position of the cation as observed in crystal coordinates. The structures for K^+, Rb^+, and Cs^+ were obtained utilizing Christiansen's relativistic effective-core-pseudo potentials (ECP) for the cation combined with the 6-31G* basis set for remaining elements. Further, for the guanine·Na^+ and guanine·K^+ complexes, we calculated the dependence of the interaction energy on the interatomic O6−M^+ distance starting from the optimized geometry and varying the O6−M^+ distance. The calculations were performed by applying the second-order Møller−Plesset perturbational method (MP2) with the 6-311+G-(d,p) basis set and corrected for the basis set superposition error. These accurate quantum chemical energies were compared with those provided by the force field. All calculations were carried out using the Gaussian94 suit of programs.[20]

(16) Pearlman, D. A.; Case, D. A.; Caldwell, J. W.; Roos, W. S.; Cheatham, T. E., III; Ferguson, D. M.; Seibel, G. L.; Singh, U. C.; Singh, P.; Weiner, P.; Kollman, P. A. AMBER 4.1, University of California, San Francisco, CA.

(17) Jorgensen, W. L.; Chandresekhar, J.; Madura, J.; Impey, R. W.; Klein, M. L. *J. Chem. Phys*. **1983**, *79*, 926−937.

(18) Harvey, S. C.; Tan, R.-K., Z.; Cheatham, T. E., III. *J. Comput. Chem.* **1998**, *19*, 726−740.

(19) (a) Cheatham, T. E., III; Kollman, P. A. *J. Am. Chem. Soc*. **1997**, *119*, 4805−4825. (b) Ferrin, T. E.; Huang, C. C.; Jarvis, L. E.; Langridge, R. *J. Mol. Graph.* **1988**, *6*, 13−27.

(20) Frisch, M. J.; Trucks, G. W.; Schlegel, H. B.; Gill, P. M. W.; Johnson, B. G.; Robb, M. A.; Cheeseman, J. R.; Keith, T.; Petersson, G. A.;. Montgomery, J. A.; Raghavachari, K.; Al-Laham, M. A.; Zakrzewski, V. G.; Ortiz, J. V.; Foresman, J. B.; Peng, C. Y.; Ayala, P. Y.; Chen, W.; Wong, M. W.; Andres, J. L.; Replogle, E. S.; Gomperts, R.; Martin, R. L.; Fox, D. J.; Binkley, J. S.; Defrees, D. J.; Baker, J.; Stewart, J. J. P.; Head-Gordon, M.; Gonzalez, C.; Pople, J. A. Gaussian, Inc., Pittsburgh, PA, 1995.

Results

3.4-ns Simulation of the All-Parallel Stranded Guanine Quadruplex Core of d(TG$_4$T). Initial coordinates were taken from the atomic (0.9 Å) resolution crystal structure of d(TG$_4$T).[4c,d] Eight quadruplex molecules exist in the unit cell of this structure, with arrangements of two parallel duplexes stacked on top of each other. At the interquadruplex junctions, guanine quartets at the 5′ ends of the guanine quartet stems stack on top of each other with 5′ to 5′ orientation of the coaxially stacked quadruplex molecules. The 5′ terminal thymine residues of each strand project away from the helical axis of the molecule and do not participate in the quadruplex motif. Rather, these thymine residues are utilized to build the three-dimensional crystal lattice.[4c] Thus, a quasi-continuous system of eight consecutive guanine quartet layers is formed that reverses its polarity at the interquadruplex junction. In the crystal, one sodium ion was found sandwiched between every two adjacent guanine quartet layers, located in the cavity formed by eight guanine O6 keto oxygens. This geometry was also found at the interquadruplex junction, resulting in a string of seven sodium (Na^+) ions that line up along the helix axis. There is some variability in the position of the Na^+ ions with respect to the O6 keto oxygens. For our studies, we used molecule 4 from the asymmetric unit of this crystal structure. Our primary aim being the investigation of the dynamic properties of the guanine quadruplex stem, we omitted both 3′ and 5′ terminal thymine residues in the simulations, leaving a guanine quadruplex core of four layers of stacked cyclically hydrogen bonded guanine quartets (Figure 2a). Strands in the simulation are denoted A−D, and residues are numbered starting from the 5′ terminal guanine residue G1 in strand A to the 3′ terminal guanine residue G16 in strand D. We initially placed a string of four Na^+ cations into the channel of the quadruplex, using the crystal data. One sodium ion thus was placed in plane of the 3′ terminal guanine quartet. Two further sodium ions are sandwiched exactly between adjacent guanine quartet layers, while one sodium ion is located below the plane of the 5′ terminal guanine quartet (Figure 2a). The latter is equivalent to the ion found between adjacent coaxially stacked quadruplexes at the 5′−5′ junction in the crystal. During the equilibration period, we observed a rearrangement of the ions. This can be seen in Figure 2b, which shows the structure after the initial equilibration period. The sodium ion previously located below the plane of the 5′ terminal guanine quartet has left its axial position and is no longer involved in coordinate bonds with the O6 guanine keto oxygen atoms. Further, the remaining three sodium ions relocated in a way to reach equidistance with respect to each other and also to the O6 oxygens of neighboring guanine residues (Figure 2b).

After equilibration, a 2.6-ns period of production simulation followed. The resulting theoretical structure was in excellent overall agreement with the crystal coordinates used as a starting model, with rmsd values between the respective structures less than 1 Å along the entire trajectory (Figure 2c). The characteristics of the guanine quadruplex structure such as all-anti glycosidic bond conformation of the guanines,[21] planarity of the quartet layers, helical twist, and interstrand distances are maintained in the theoretical structure. This is illustrated in Figure 2d, which shows a stereo overlay plot of the respective crystal and theoretical coordinates. Highest rms deviations were found for phosphates (rmsd 1.1 Å), and a pronounced positional shift occurred close to the 5′ terminus of one strand, where a phosphate group underwent a sudden conformational transition at around 1.8 ns (Figure 2d, arrow), affecting only the γ and α angles along the phosphodiester linkage.[22] This positional perturbation did not propagate to adjacent ribose rings of the sugar phosphate backbone. The groove width of the simulated structure is somewhat larger with interphosphate distances increasing by around 1 Å compared to the crystal coordinates. In the crystal structure, most of the sugar rings adopt a C2′-endo pucker while several others are puckered C1′-exo, with an average pseudorotation angle of 156°. The simulated structure shows sugar puckering shifted toward C1′-exo, with an average pseudorotation angle of 122°. The most likely reason for this discrepancy is the defect of the force field used, since it prefers lower pucker values compared to experimental structures also for B-DNA.[11i,q] This point has been extensively discussed in the literature.[11i,q]

The base positions remained largely constant along the trajectory (rmsd 0.6 Å). Nevertheless, we observed local differences in the cyclic hydrogen bond geometries of the guanine quartets in the theoretical structure as compared to the crystal coordinates, in particular in the central two quartet layers. In the inner quartets of the simulated structure, the guanines are shifted with respect to each other such that bifurcated hydrogen bonds are formed with equidistant bond lengths (around 3.3 Å) between the N1 nitrogen of one guanine and the N7 and O6 atoms of the adjacent guanine residue. Geometries of the outer two quartets are closer to the crystal coordinates and show no bifurcated hydrogen bonding (Figure 2e). As will be explained below, the bifurcated bonding is likely to be an artifact of the pair additive nature of the force field neglecting polarization effects for cation−base interactions. The theoretical quartets are symmetrical with diagonal O6−O6 separations of 4.0 Å for inner and 4.3 Å for outer quartets. This is in agreement with the crystal data showing symmetrical quartets except that the O6−O6 separation in crystal is around 4.5 Å (for all quartets). During the entire production simulation, the sodium ions remained located between the quartet layers.

Figure 2f shows the most localized sites of hydration of the parallel G-DNA stem as revealed by our simulation. The average structure over the last 1 ns of simulation is displayed, contoured at 20.0 hits per $(0.5\ A)^3$ grid element, which is equivalent to regions with ca. 4.9 times the bulk water density.[19] Highest water densities are observed in the grooves, and the hydration pattern is qualitatively consistent with the spine of single water molecules observed in the high-resolution crystal structure.[4c] All the grooves are equivalent and relatively narrow, leading to highly localized water molecules. The spine of the hydration is visible even at higher contour levels. The densities in the area between the first (5′ end) and the second quartets are very well developed even at 50 hits per grid element (∼12.0 bulk density),[19] when no other densities can be identified (not shown). Closer inspection of the water densities reveals two favorable water positions. The first one is between adjacent quartets, and the water molecules positioned here interact mainly with the guanine N3 position (O−N3 distance is 2.9 Å) and the N2 group of adjacent guanine (in the same strand; O−N2 distance 3.5 Å). The second position is in the plane of the quartet, and the water molecules interact primarily with the guanine N2 group. Altogether the N2 position appears to be the most hydrated site which is in agreement with the crystal data.[4c] Another quite well developed site of hydration besides the grooves is the

(21) The average χ values for individual quartets (calculated along the entire trajectory) were 201° for the 5′ terminal quartet, 242° for 3′ terminal quartet, and 228° for the inner quartets. The corresponding values in the crystal structure are around 238° for the 5′ terminal quartet and around 250° for the other quartets.

(22) A very fast and concerted change of two angles occurred: the γ torsion changed from 55° to 190° and α from ca. 290° to 110°.

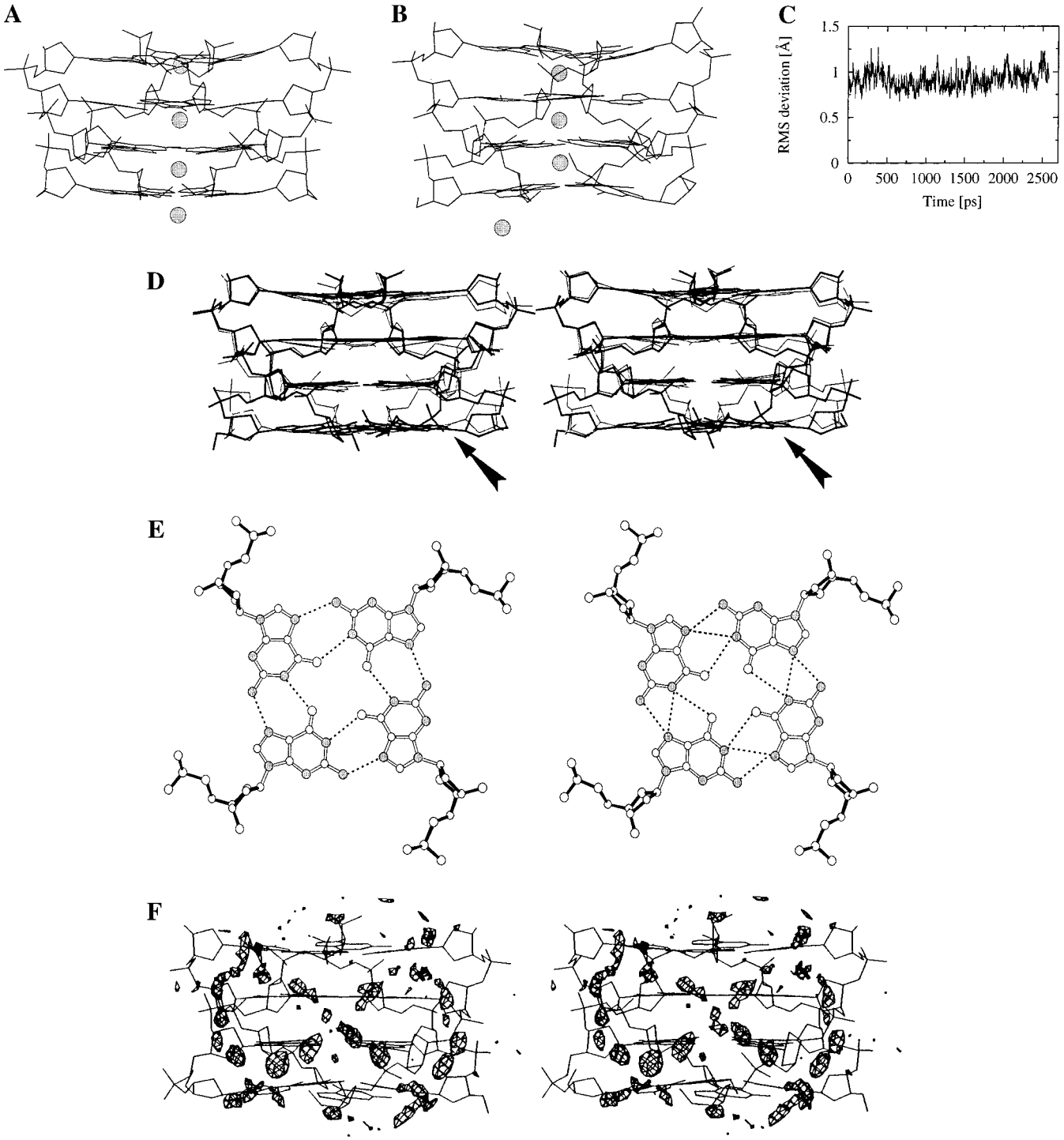

Figure 2. (A) Simulation of parallel d(G_4). (A) d(G_4) coordinates from the 0.9 Å crystal structure.[4c−e] 5′ and 3′ terminal thymine residues were omitted in the simulations. Four sodium cations in the central ion channel are shown as larger spheres. (B) d(G_4) structure after equilibration. One ion at the 5′ terminus has left the vicinity of the DNA molecule (bottom). (C) Evolution of rmsd values along the trajectory. (D) Stereo overlay plot of the final averaged simulated structure (solid black lines) and the crystal coordinates (thin lines). A phosphate group (arrow) adopting an alternative stable position in the theoretical structure is indicated by an arrow. (E) Guanine quartet geometries in the simulated structure. The two outer quartets both at top and bottom of the molecule show two hydrogen bonds each between adjacent guanine residues (left). The inner quartets are slightly shifted, giving rise to bifurcated hydrogen bonds involving guanine N1, N7, and O6 atoms (right). **(**F) Hydration of the parallel G-DNA stem. Stereoview of the averaged structure from the last nanosecond of the simulation (with three Na^+ in the channel). Water oxygen densities are displayed at a contour level of 20.0 hits per (0.5 A)^3 grid element, consistent with ca. 4.9 times bulk water density in these regions.[19]

entrance of the G-stem channel, which is in agreement with the Strahan et al. NMR/MD study.[5e] The hydration of the phosphate group regions is not clearly visible. This does not indicate a lack of hydration. Rather, the water positions in these regions are sterically less restricted so they are not that well-localized.

Recent MD studies reported an extensive intrusion of monovalent cations into the spine of hydration in the minor groove of B-DNA.[11d] In our simulation, we have seen few occasions when a nonchannel cation was temporarily coordinated (on a scale of 10−100 ps) to a guanine of one of the outer quartets in a position above or below the stem groove,

being closer to the N2 (below 3 Å) than to N3 nitrogen. This position can be considered as an extension of the spine of hydration; however, throughout the whole simulation, we did not see any intrusion of the Na^+ cations into the central part of the spine of hydration (i.e., into a position within the groove between two consecutive quartets). Thus the intrusion of cations into the spine of hydration of G-DNA stem does not seem to be significant, in contrast to B-DNA.

Due to space limitation, we do not intend to discuss the hydration of our simulated molecules in the present contribution in more detail and a comprehensive analysis of hydration of all four-stranded G-DNA and i-DNA molecules will be reported in a separate study.

To further test the stability of the structure, simulation was extended by 0.8 ns at an elevated temperature of 400 K. However, no alterations were observed during this period.

Molecular Interactions Parallel to the Helical Axis of the d(G_4) Quadruplex. The vertical interactions in the guanine quadruplex consist of three components: base stacking, ion−ion interactions between Na^+ cations in the central channel, and interactions between the ions and flanking[23] guanine quartets. We have calculated the vertical interactions for three systems: First, we investigated a structure with two adjacent stacked guanine quartets without cations. Second, we chose two stacked guanine quartets with two Na^+ cations located exactly between consecutive quartets (compare Figure 2a, out-of-plane position).[23] Third, we investigated a hypothetical structure consisting of two layers of guanine quartets with one Na^+ ion in plane of each of the two quartets, based on the geometry observed for the 3′ terminal guanine quartet layer in the d(TG_4T) crystal structure. Calculations were carried out utilizing the Cornell et al. force field assuming a dielectric constant of 1 to evaluate in vacuo vertical interaction energies.[24] The stacking energy consists of two terms: van der Waals and electrostatic. The van der Waals contribution was found to be stabilizing and yielded values between −45 and −49 kcal/mol, depending on the cation position. The structure without cations had an electrostatic contribution of +28 kcal/mol. Thus, the energy provided by base stacking amounts to −21 kcal/mol. Inclusion of two cations obviously increases the electrostatic contribution due to charge−charge repulsion between the Na^+ cations. However, this is compensated for by stacking interactions between the cations and the guanine quartets between which they are sandwiched. The energy terms for electrostatic stacking interactions were calculated at +12 kcal/mol for out-of-plane position of cations and +42 kcal/mol for the cation in-plane position. The corresponding total stacking energies are −34 and −8 kcal/mol, respectively. Thus, the vertical interactions are attractive in all configurations.[25]

We also performed calculations with a dielectric constant adopting a value equal to the interatomic distance in angstroms. This procedure was applied in numerous theoretical studies in an attempt to mimic the effect of solvent screening. According to this model, the total stacking energies are −37 kcal/mol for stacked guanine quartets without cations, −66 kcal/mol with out-of-plane cation positions, and −42 kcal/mol for cations arranged in plane of the guanine quartets, respectively. While this solvent effect estimate is rather crude and probably overestimated,[26] it nevertheless shows that solvent screening reduces electrostatic repulsion, as expected. Solvent effects are much more accurately approximated during MD simulations using explicit solvent molecules.

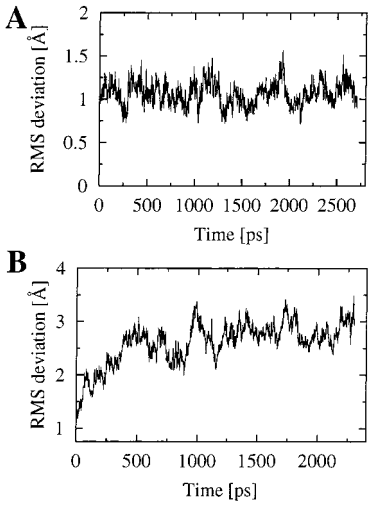

Figure 3. Evolution of the rmsd values along the trajectory in simulations with two sodium cations (A) and without ions (B) in the central ion channel of the parallel quadruplex.

Molecular Dynamics of the All-Parallel d(G_4) Guanine Quadruplex with Two Na^+ Cations in the Central Channel. We carried out a 2.7-ns production simulation of a d(G_4) quadruplex where the Na^+ cations were initially removed from the molecule. However, two Na^+ cations were positioned along the helical axis of the molecule both above and below the terminal guanine quartets of the quadruplex stem. During the equilibration period, they shifted their positions into the cavities between the terminal two guanine quartets of the molecule at either end of the quadruplex stem, where they came to rest in an out-of-plane arrangement at equidistance from the respective O6 guanine keto oxygens. The central cavity was initially unoccupied. During the subsequent simulation, the rms deviation between the crystal data and the theoretical structure reached somewhat higher values compared to the previous simulation with three Na^+ ions, but did not exceed 1.2 Å (Figure 3a). Again, the simulated structure remained stable and close to the crystal coordinates along the trajectory, with two ions apparently sufficient to provide enough electrostatic stabilization of the molecule. More frequent motions of individual phosphate groups were observed during this calculation, along with minor positional shifts of ribose sugar rings in some cases. However, the major alteration we observed during production simulation involved a redistribution of the ions in the channel of the quadruplex. The Na^+ cation that was located between the 5′ terminal guanine quartet layers of the molecule after equilibration suddenly jumped into the previously unoccupied central cavity of the quadruplex. This transition occurred very rapidly at 1.4 ns, and the cation did not spend any time in the plane of the quartet. The trajectory of the second cation in the structure is not affected by this event, indicating that the charge−charge repulsion between the two cations is sufficiently screened. Bifurcated hydrogen bonding of inner quartet layers as described

(23) It means that the interaction of a cation with its closest G-quartet is not considered as a contribution to vertical interactions. Thus the calculations were carried out such that the stabilization between the cation and its own (closest) quartet was not included. In other words, we calculated the energy of the following "dimers": (Na^+ + 4G)···(Na^+ + 4G), thus obtaining numbers comparable to base stacking energies in other nucleic acid structures.

(24) Due to the pair additivity of the force field, this term equals to the exact value of the vertical interaction energy even after adding solvent. The AMBER force field provides a rather reasonable estimate of base stacking energies and has been extensively tested in this respect.[10]

(25) The net base pair stacking energy amounts to −10 to −15 kcal/mol in B-, Z-, and A-DNA double helices[9a] while this contribution is repulsive, +30 kcal/mol in i-DNA.[14]

(26) Friedman, R. A.; Honig, B. *Biopolymers* **1992**, *32*, 145−159.

Table 2. Interaction Energy ΔE (kcal/mol) between Guanine O6 and Na^+ and K^+ Metal Ions Depending on the O6−M^+ Distance (Å)[a]

monovalent metal ions M^+	O6−M^+ distance (Å)	ΔE_{MP2} (kcal/mol), ab initio	ΔE_{AMB} (kcal/mol), emp potential
Na^+	1.749	−10.0	+69.5
	1.849	−21.2	+20.8
	1.949	−27.6	−2.3
	2.049	−30.9	−12.8
	2.149[b]	−32.2	−17.3
	2.349	−31.5	−19.0
	2.549	−28.8	−17.6
	2.749	−25.5	−15.6
K^+	2.288	−14.5	−5.8
	2.388	−17.8	−10.9
	2.488	−19.6	−13.1
	2.588[c]	−20.3	−14.0
	2.788	−20.0	−13.8
	2.988	−18.4	−12.6
	3.188	−16.6	−11.3
Li^+	1.746[b]		
Rb^+	2.761[c]		
Cs^+	2.899[c]		

[a] Optimal O6−M^+ distances of other Ia group ions are shown for comparison. The M−O6−C6 angle was frozen at 135°. [b] Optimal O6−M^+ distance obtained by the HF/6-311+G(d,p) method. [c] Optimal O6−M^+ distance obtained by the HF/6-31G(d)+ECP method.

in the simulation with three cations was not observed here in periods when a guanine quartet is in contact with one cation only. Then, the averaged base pairing geometry closely resembles the pattern observed in the crystal. No further changes were observed during this trajectory. Interestingly, the outer cavity was filled by water all the time while being unoccupied by a cation. This observation strongly supports a genuine view that hydrogen bonded guanine quartets are never left vacant in G-DNA. Of course, a central cavity in the stem is not hydrated when surrounded by cations from both sides, which does not allow water molecule to enter the empty cavity on our time scale.

Ab Initio Calculations of Guanine−Na^+ and Guanine−K^+ Interactions. The distribution of Na^+ cations in the above MD simulations strictly avoids in-plane positions of the cations with respect to the G-quartets (in contrast to the crystal data). This indicates an overestimation of the short-range repulsion between the cation and the O6 keto oxygen atoms of guanine bases. This could trap the cations between the quartet layers and restrain their mobility in the channel. Therefore, we compared the empirical potential data for a complex between Na^+ or K^+ and guanine with reliable data obtained by the ab initio quantum-chemical method. The results are listed in Table 2, showing that the empirical potential covers only 60% of the actual binding energy between guanine O6 and Na^+.[27,28] The difference between the ab initio and empirical potential data is 13 kcal/mol. Further, the potential clearly overestimates the optimal O6 − Na^+ distance by 0.25−0.3 Å. Similar calculations carried out for K^+−guanine interaction also show a pronounced discrepancy between ab initio and empirical potential data. The interaction energy is underestimated by ca. 30%, i.e., by 6 kcal/mol. In contrast to Na^+, however, the potential reproduces the optimal O6−K^+ distance. These results are not surprising and are in line with the quantum mechanical studies on cation−base interactions.[28] The discrepancy originates in the neglect of "nonelectrostatic" contributions such as polarization by pair-additive potentials.[28] This defect is inherent to all pair-additive force fields, and we must underline that it cannot be repaired by varying parameters (cation radius, well depth) of such force fields since the potential energy function does not include appropriate terms to do so. Inspection of Table 2 clearly shows that the discrepancy for Na^+ is larger than for K^+; thus, even the relative difference between the two cations is not properly approximated.

Molecular Dynamics of the Parallel d(G_4) Guanine Quadruplex with Reduced Cation Radii. We chose to carry out a 2-ns simulation with the van der Waals radius of the Na^+ cations in the channel reduced by 0.25 Å and unchanged potential well depth. We used the same starting structure with four cations in the channel as for the first 3.4-ns simulation. This simulation also produced a stable trajectory with an rmsd value of 1.0 Å. However, we observed altered cation mobilities. During equilibration, the cation localized in the crystal below the plane of the 5′ terminal guanine quartet (Figure 2a) moved into a position in plane of this quartet. The cation localized in an in-plane position at the center of the 3′ terminal quartet in the crystal relocated above the plane of this quartet and shortly (200 ps) after left the vicinity of the quadruplex molecule entirely. The remaining two cations redistributed during the simulation in a way that they occupied the cavities between the three guanine quartet layers toward the 3′ end of the guanine quadruplex stem. During the simulation, the cation associated with the 5′ terminal quartet was largely localized in plane of this quartet where it had moved after equilibration. More specifically, this cation was found in the in-plane position for intervals of 0.2−0.3 ns during simulation while for brief intervals (0.05 ns) between it relocated to a more central position into the cavity between the 5′ terminal two guanine quartets of the quadruplex. Thus reduction of the radius of the cations improved the mobility of the cations in the channel. However, we still observed clear bifurcated hydrogen bonding between guanines of the inner quartet layers and this structural feature is not influenced by reducing the cation radius.

Molecular Dynamics of the d(G_4) Guanine Quadruplex without Cations in the Central Channel. Next, we removed all Na^+ cations from the central channel of the quadruplex. The system was neutralized by adding these cations to phosphate groups of the molecule. After equilibration, 2.3 ns of production simulation was performed. The channel was fully hydrated within the first 100 ps and remained hydrated throughout the whole simulation. The theoretical molecule showed large perturbations with rmsd values with respect to the crystal reaching 2.6 Å (Figure 3b). In the period up to 0.5 ns, one 3′ terminal guanine residue (G16 of strand D) developed a pronounced propeller twist and started to buckle out of the guanine quartet plane. This initiated a shift of the entire strand D. The base pairing interactions between strands A and B, B and C, and also C and D were basically maintained, with the bases of strand C showing large propeller twist angles. However, we observed a slippage of the base pairing interactions between strands D and A. Ultimately, the 5′ terminal guanine G16 from strand D, which was previously engaged in pairing interactions with guanine G4 from strand A in the 5′ terminal guanine quartet of the quadruplex, was found to form hydrogen bond interactions

(27) The total error in empirical potential cation−ligand association energies appears to be reduced at first glance when more ligands are included, with the force field underestimating the cation−ligand attraction while at the same time neglecting polarization interligand repulsion. Nevertheless, the balance between cation−ligand and interligand contributions, as evaluated by the potential, remains poor. The difference for the monovalent Na^+ ion is still comparatively small. Larger differences would arise for divalent cations, as polarization effects are stronger, and for transition metals where substantial charge transfer occurs.[28]

(28) Šponer, J.; Burda, J. V.; Sabat, M.; Leszczynski, J.; Hobza, P. *J. Phys. Chem. A* **1998**, *102*, 5951−5957 and references therein.

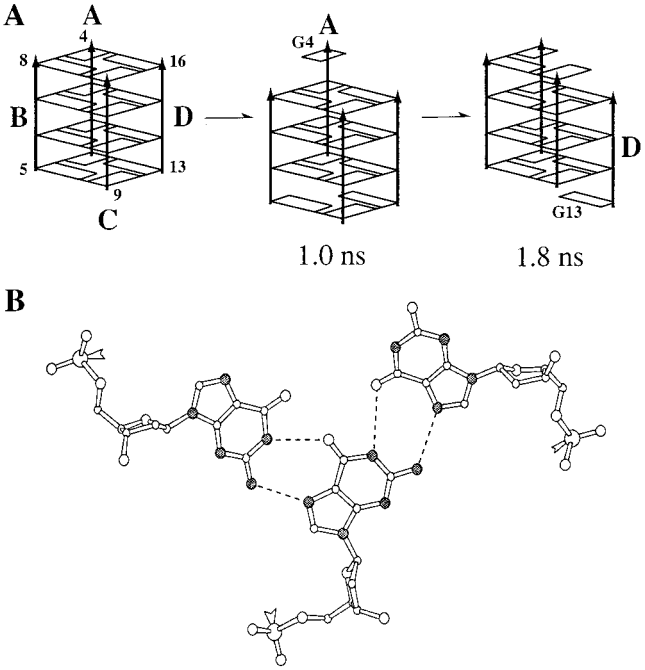

Figure 4. Structural dynamics of the d(G_4) molecule. "Walking" of a strand in the parallel quadruplex without ions in a schematic drawing. The starting geometry is shown on the left. Strand polarity from 5′ to 3′ is indicated by arrows. Strands are labeled A−D, and first and last residues in strands are denoted. Guanines are shown as open boxes. All residues are in the anti conformation. At 1.0 ns, a slipped structure appears (50 ps) with one guanine triad at the 5′ terminus and an isolated guanine residue G4 from strand A at the 3′ end (center). At 1.8 ns, a further rearrangement occurred (100 ps), giving rise to a slipped structure with a triad at the 3′ end and one isolated residue G13 from strand D at 5′. The guanine triad involved is shown in a ball-and-stick representation below (nitrogen atoms are shaded).

with residue G3 from strand A. This "out of register" base pairing propagated along strand D, leaving guanine G4 unpaired. The bases fluctuated between this new, dislocated structure and the original positions without ever recovering the starting geometry. This structure has some resemblance to a spiral and is very transient and flexible.

Further rearrangements of the spiral intermediate structure occurred at around 1.0 ns of simulation and lasted approximately 50 ps. We observed a system of three guanine quartets enveloped by an isolated residue (G4) at the 3′ terminus and a 5′ terminal triad of three mutually hydrogen bonded guanine residues. The rearrangement can be described in simple terms as strands B and C basically following the initial slippage of strand D leaving strand A one base step behind. At 1.8 ns, another rearrangement occurred lasting approximately 100 ps. Here, again, a triad could be observed; however, this time at the 3′ terminal end encompassing the 3′ terminal guanines from strands A, B, and C. Now, guanine G13 from strand D had lost its hydrogen bonding partners though it remained stacked on the adjacent quartet. Here, strand D appears to have shifted by one base step. The described rearrangements are illustrated in a schematic fashion in Figure 4.

After 2.3 ns we elevated the temperature of the system to 400 K with the aim to increase the mobility of cations such that some of them could eventually reach the channel area. However, this led to a complete disintegration of this structure in contrast to the ion stabilized structure described above that maintained its geometry even at 400 K.

MD Simulations of the Guanine-Rich Parallel d(G_4) "Walking Structure" Consisting of Three Guanine Quartets and One Guanine Triad. We investigated the influence of a repositioning of sodium ions on the geometrical evolution of the "slipped" structure we had observed during the preceding simulation without cations in the central core of the molecule. The structure we selected as a starting model had occurred at 1.9 ns in that calculation and showed strand D slipped with respect to the remaining strands with its 5′ terminal guanine G13 isolated, and a triad formed at the 3′ terminus (see above). We placed one Na^+ ion in the cavity between the triad and the adjacent guanine quartet layer. A second Na^+ ion was placed in an in-plane position into the center of the 5′ terminal guanine quartet layer. During the equilibration period, the ions were redistributed, occupying the two cavities formed by the three adjacent intact guanine quartet layers in the molecule (Figure 5a). After equilibration, a 3.0-ns period of production simulation was performed. We observed a quick stabilization accompanied by a drastic reduction of fluctuations of the structure with the D strand shifted. During simulation, we observed further relocation of the ions in the central channel of the molecule. After 0.4 ns, the cation in the molecule center (Figure 5b) moved back to its preequilibration position between the triad and the adjacent guanine quartet layer, leaving the central cavity of the molecule unoccupied. This cavity was filled at 0.8 ns, with the other ion situated between the two 5′ terminal guanine quartets moving up and into the center of the molecule. Now the gap between the quartets near the 5′ terminus remained vacant. The ions remained in their new positions until the end of the simulation.

We have evaluated separately the rmsd values of the four individual strands in the final product of our simulation with respect to their crystal counterparts, thus canceling out the positional discrepancies that are due to the vertical dislocation of strand D only. We obtained low rmsd values (around 1.0 Å) for strands A−C. A rather high value, 2.6 Å, was obtained for strand D, which had "walked" parallel to the helical axis. Thus, strands A−C had essentially recovered the geometry observed in the crystal. The high rmsd value for D, on the other hand, is not a consequence of the vertical shift but stems from the deformation of this strand. Compared to the crystal coordinates, this strand is underwound. More precisely, two D strand residues, G16 and G15, are in similar positions as in the crystal, while residues G14 and G13 are rotated by approximately 75°. Guanine G13 is the isolated base stacked on the 5′ terminal guanine quartet.

After the last redistribution of cations, we noticed that guanine G9 of the 5′ terminal guanine quartet became unstacked and began to progressively bend out of the plane of the 5′ terminal quartet layer until it reached a position where a hydrogen bond was formed between its O6 keto oxygen and the N2 amino group of the isolated guanine G13 residue (Figure 5c). Only one hydrogen bond interaction from the N2 amino group of guanine G9 to the N7 nitrogen of guanine G5 was maintained from the set of interaction that had previously stabilized residue G9 in the 5′ terminal quartet layer. Upon reaching this geometry with actually only two intact guanine quartets remaining, we decided to add a third cation to the structure into the vacant cavity between this now geometrically perturbed quartet layer and the 3′ adjacent still intact guanine quartet. Ensuing simulation immediately led to a full repair of the 5′ terminal quartet layer during equilibration. Two nanoseconds of production simulation did not lead to any destabilization of either the 3′ terminal guanine triad or the three intact quartet layers, and the

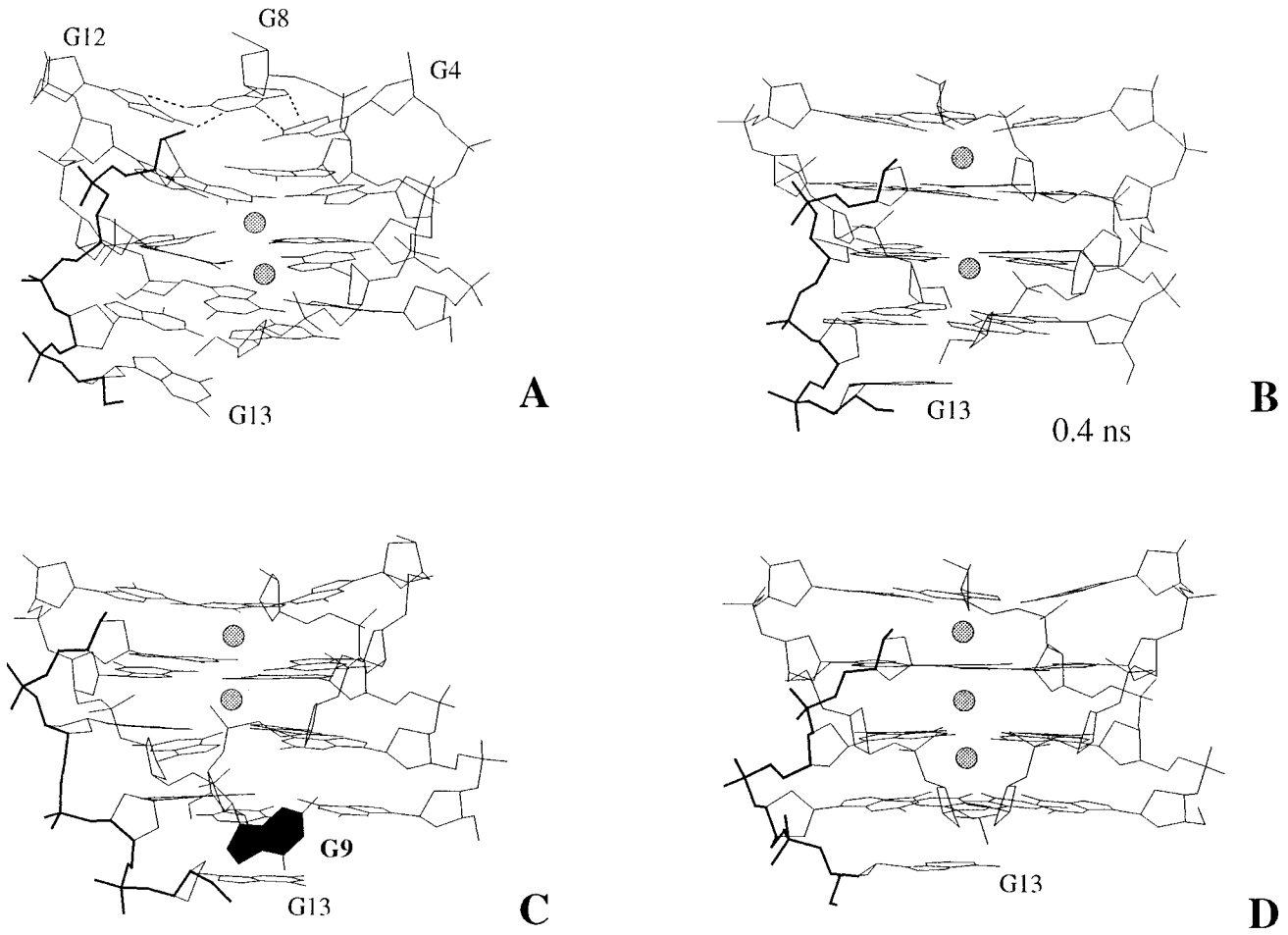

Figure 5. (A) Structure with guanine triad (top, dashed lines), isolated G13 residue (bottom), and two sodium ions in the ion channel after equilibration. The molecule is slightly tilted toward the reader in panel A. The backbone of strand D is drawn with thick lines. (B) Redistribution of ions in the structure at 0.4 ns in this simulation. (C) Residue G9 in the 5′ terminal guanine quartet becoming unstacked and looping out of the plane of this layer to interact with isolated residue G13. (D) Addition of a further cation repairs the 5′ terminal quartet layer, yielding a nanosecond-stable structure with one triad, three quartets, one isolated base, and three integral sodium ions.

isolated residue guanine G13 remained stacked on the molecule. The rmsd values of the three intact quartet layers (calculated as above) were 0.5 Å with respect to the crystal coordinates, and rmsd values of strands A−C were 0.8 Å. The largest rms deviation (1.6 Å) was found for strand D which had "slipped", mainly due to a different position of the isolated residue G13. The final structure (Figure 5d) was again very stable and rigid, and only small positional fluctuations were observed.

2.5-ns MD Simulations of the Antiparallel d($G_4T_4G_4$) Oxytricha Telomeric DNA Quadruplex with Na^+ and K^+, Crystal Coordinates as Starting Model. Coordinates for this simulation were taken from the crystal structure of the antiparallel guanine quadruplex solved at 2.3 Å resolution.[4a] The quadruplex structure is formed by two oligonucleotide strands with the sequence d($G_4T_4G_4$). In the crystal, the strands fold back on themselves forming hairpins and associate via their guanine containing parts to form a quadruplex stem stabilized by four layers of cyclically hydrogen bonded guanine quartets stacked on top of each other (Figure 6a). This four-stranded guanine stem is capped at either end by four-nucleotide loops formed by the four thymine residues from each hairpin. The loops thus reach across the edges of the stem, each loop across one groove. In contrast to the all-parallel d(G_4) quadruplex, the strand orientation of adjacent strands is antiparallel. Furthermore, glycosidic bonds here alternate between anti and syn in the guanine rich stem both along the covalent linkage as well as in the plane of the quartet layers (Figure 6a). In the 2.3-Å crystal structure, only one cation (K^+) was tentatively localized and interpreted as occupying a disordered position between the central two guanine quartet layers.[4a] In our simulations, in contrast, we decided to place three cations into the cavities of the guanine rich stem of the molecule similar to the situation described above for the all-parallel d(G_4) structure. Two 2.5-ns simulations were carried out. During one simulation, Na^+ cations were placed in the central channel of the quadruplex, while larger K^+ cations were tested in the other.

The simulations provided both for Na^+ and K^+ cations stable trajectories with low geometrical fluctuations (Figure 6b,c). The cations placed into the channel remained in position along the whole trajectory.[29] The overall geometry of the guanine bases was well-conserved including the alternating anti and syn glycosidic bond conformations.[30] We observed minor differences in the behavior of the guanine quadruplex stems during the simulations carried out with Na^+ or K^+, respectively. The guanine quartets in the Na^+ simulation showed the same pattern of bifurcated hydrogen bonds between guanine residues as described above for the all-parallel d(G_4) structure. Pronounced

(29) One exception occurred during the "Na^+" simulation, where once one of the outer cations tested a position outside the channel entrance. The whole event, however, took just 5 ps.

(30) In fact, the first guanine residue in the crystal is anti ($\chi = 135°$) while it should be syn. This has been swiftly repaired in both simulations by switching to the genuine syn arrangement (χ ca. 45°).

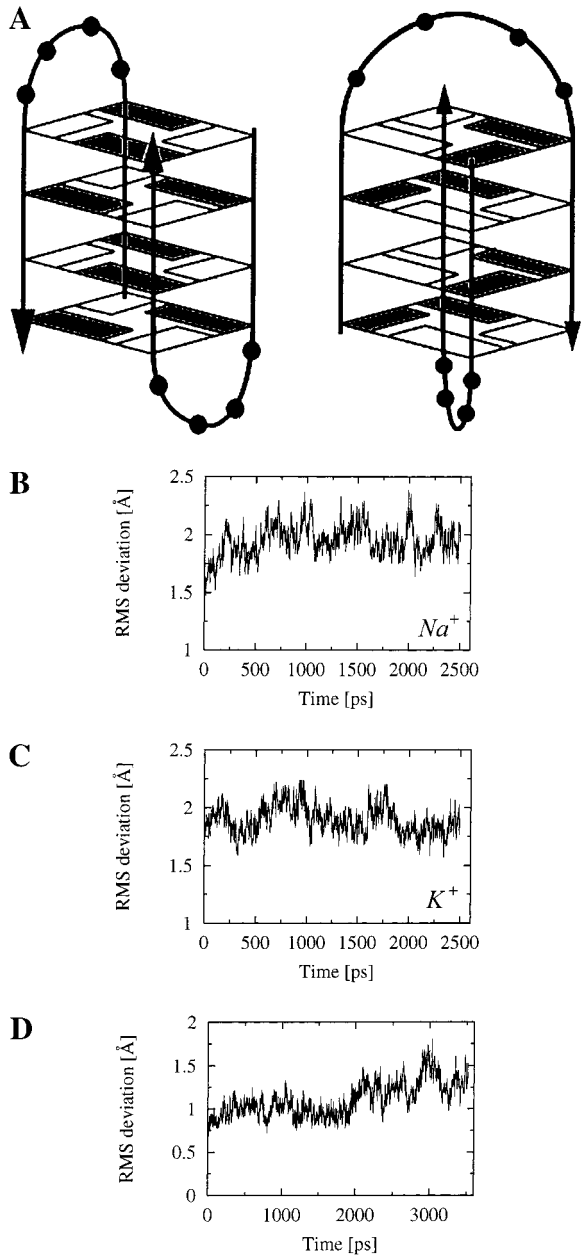

Figure 6. MD simulations of *Oxytricha* telomeric DNA d($G_4T_4G_4$). (A) Conformations of d($G_4T_4G_4$) derived from crystallographic studies[4a] (left) and NMR experiments[4b] (right). Strand polarities are indicated by arrows. Guanine residues are shown as open (anti) or shaded (syn) boxes (cf ref 4f). Thymines are drawn as black spheres. The molecule in the crystal shows edge-looped geometry while the NMR model has diagonal four-thymidine loops. (B) Evolution of the rms deviations (guanine stem only) throughout the Na^+ simulation based on edge-looped crystal coordinates. (C) The same as panel B for the simulation with K^+. (D) Evolution of the rmsd value of the guanine stem during simulation of the diagonal-looped structure, NMR model as starting coordinates.

bifurcation did not occur in the simulation with larger K^+ ions (N1−O6 distances around 3.2 Å and N1−N7 distances around 3.5 Å, respectively). All theoretical quartets were symmetrical with O6−O6 distances around 4.3 Å for the outer and around 4.0 Å for the inner layers for the Na^+ simulation (similar to the parallel structure). These distances increase by 0.3−0.4 Å in the course of the K^+ simulation. In contrast, the experimental O6−O6 distances vary from exceptionally tight (2.6 Å) to up to 6.2 Å.

The rmsd values of the theoretical structures as compared to the initial crystal coordinates used as a starting model were rather significant, that is 2.9 Å (Na^+) and 2.5 Å (K^+) for the entire structure, respectively. The rms deviation for the guanine stem without the thymine residues in the loops was around 1.9 Å in both calculations, which is still significantly higher than in the simulations of the all-parallel d(G_4) molecule described above. Actually, the rms deviation of the guanine quadruplex stem in the antiparallel d($G_4T_4G_4$) structure reached its final value already during the initial equilibration. In the crystal structure, several quartet layers of the quadruplex stem adopt a somewhat irregular geometry. Thus, some of the guanine residues are considerably buckled and paired guanine bases exhibit high propeller twist values. During the equilibration period, the guanine quartet layers in the theoretical structure quickly relaxed into a largely regular planar arrangement. The quartets are in fact closer to those found in the atomic resolution crystal structure of the parallel d(TG_4T) quadruplex (0.5 Å rmsd) than to the d($G_4T_4G_4$) crystal coordinates used as a starting model (rmsd around 0.8 Å).

The antiparallel guanine quadruplex as observed in the d($G_4T_4G_4$) crystal structure has two wide and two narrow grooves with interstrand phosphorus−phosphorus distances measuring from as close as 3.9 Å to up to 12.1 Å, respectively. The interphosphate distances in the averaged simulated structures however are more uniform. More precisely, the closest interphosphate distances measure on average[31] 8.6−11.9 Å across the narrow grooves and 11.1−14.1 Å across the wide grooves. The closest interphosphate distance that occurred at any time during the simulation was 5.2 Å in the narrow grooves and 8.5 Å in the wide grooves. A sterically extremely tight contact of 3.9 Å was not reached along the entire trajectory. During the simulation, positional oscillations of isolated phosphate groups were observed along the trajectories similar to those described before for the all-parallel d(G_4) quadruplex, again not affecting the geometry of adjacent ribose sugar rings apart from some more pronounced movement at the stem loop junctions.

The crystal structure of d($G_4T_4G_4$) shows two four-thymidine loops (Figure 6a). The first and fourth thymine residues of each loop are immediately adjacent to the guanine quadruplex stem and stack on top of the outermost guanine quartet layers. While being arranged in a coplanar fashion and in close proximity, they do not form hydrogen bonded pairs in the crystal. The two loops in the crystal structure are not equivalent. The major difference is that, in one loop, all four thymine residues adopt an anti glycosidic bond conformation ("all-anti" loop). In the other loop, the fourth thymine has an energetically less favorable syn conformation while the remaining three thymine residues are in anti ("syn" loop). We did not find any obvious crystal-packing constraints causing the respective thymine to adopt a syn conformation. However, in previous studies on thymines in loops of B-DNA stem hairpin structures, intermediates between syn and anti have been observed or an equilibrium between the two conformations exists.[32] Thus, the energy difference between syn and anti conformations in pyrimidine nucleotides is not insurmountable, in particular in the loops. In fact, studies on Z-DNA showed that in crystals of the Z-

(31) This means a range of closest interphosphate distances in structures averaged over three subsequent 0.5-ns intervals in both simulations, starting at 0.5 ns.

(32) Wolk, S. K.; Hardin, C. C.; Germann, M. W.; van de Sande, J. H.; Tinoco, I., Jr. *Biochemistry* **1988**, *27*, 6960−6967.

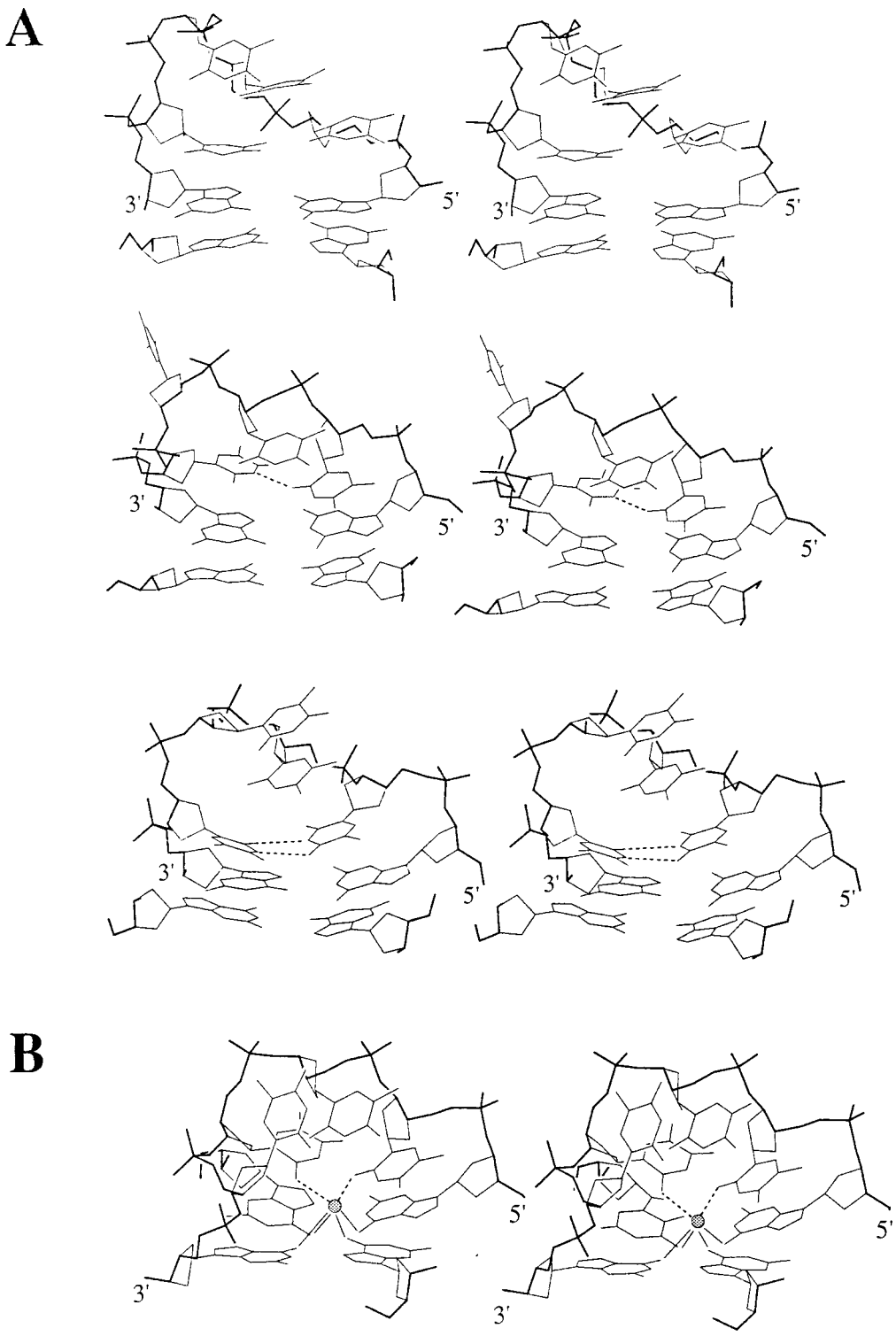

Figure 7. Structural dynamics of four-thymidine loops. (A) Stereo line drawing of four-thymidine loops and the adjacent guanine quartet in the edge-looped structure. Top: "syn" loop as seen in the crystal structure. Middle: The same loop in the Na^+ simulation with a hydrogen bond (dashed line) in a T−T base pair with one thymine syn, the other anti, and a looped-out apical thymine residue. (The K^+ simulation does not lead to looping out of the thymine; not shown.) Bottom: The other four-thymidine loop ("all anti" loop) with two hydrogen bonds in a T−T base pair (K^+-simulated structure, Na^+ simulation leads to a similar geometry). B: Stereo drawing of the stem-loop junction in the simulated diagonal-looped molecule (based on the NMR model) showing a sodium ion (larger sphere) that has left the central ion channel. Coordinate bonds to guanine carbonyl oxygens and the ion are drawn as thin black lines. Coordinate bonds to thymine carbonyl oxygens are shown as dashed lines.

hexamers d(*CGAT*CG) (*C: methylated or brominated cytosines) the thymine residues adopted the energetically less favored syn conformation even in a duplex stem.[33]

(33) Wang, A. H.; Gessner, R. V.; van der Marel, G. A.; van Boom, J. H.; Rich, A. *Proc. Natl. Acad. Sci. U.S.A.* **1985**, *82*, 3611−3615.

Both four-thymidine loops exhibited significant positional plasticity during the simulations (Figure 7a). Interestingly, the two thymine residues that are in close proximity formed hydrogen bonded T−T pairs in both loops. The first and fourth thymines of the "all-anti" loop formed already during both

equilibrations an asymmetric pair with respective O2−N3 and N3−O4 distances of around 2.9 Å, consistent with preceding in vacuo energy minimizations.[5b,e] The corresponding pair in the "syn" loop formed in the early stages of both production simulations. Here, due to the fact that one thymine involved in the T−T self-base pair is anti and the other syn, only one O2−N3 hydrogen bond is formed between the residues. The hydrogen bonded T−T pairs remain stable during the entire simulations, and the aromatic rings of the thymines involved are stacked on top of the base heterocycles of the adjacent guanine residues. The loop hydrogen bonding interactions formed very quickly during our simulations, and taking into account previous reports,[34] the formation of the T−T pairs is apparently favorable (rendering their absence in the crystal somewhat puzzling). The two independent simulations (Na^+ and K^+) provided similar geometries of the "all-anti" loop, with an rmsd value of 2.3−2.4 Å with respect to the crystal loop geometry. The rmsd value between the two simulated "all-anti" loops was 1.3 Å. In the "syn" loop, however, the third thymine residue became unstacked in the simulation with Na^+ ions and eventually projected away from the remainder of the loop, thus leading to a rather large (3.5 Å) rmsd value compared to the respective loop geometry in the crystal. A transition of this kind did not occur in the simulation involving K^+ ions (respective rmsd value for "syn" loop was 2.4 Å). As a result, the rmsd value for the geometries of the "syn" loop that were obtained in the Na^+ and K^+ simulations was 2.6 Å when compared to each other.[35]

3.5-ns MD Simulation of the Antiparallel d($G_4T_4G_4$) Quadruplex, NMR Structure as the Starting Model. We further investigated an alternative conformer of d($G_4T_4G_4$) *Oxytricha* telomeric DNA that was derived from nuclear magnetic resonance (NMR) studies.[4b] This conformer is also formed by two d($G_4T_4G_4$) oligonucleotide sequences. In contrast to the crystal structure, however, the strands do not fold back on themselves prior to association into a quadruplex. Rather, the quadruplex is formed by pairing of the DNA strands in a way that the four-thymidine loops arrange diagonally across the guanine stem on either end of the molecule (Figure 6a). Thus, opposite strands are antiparallel while individual strands have both parallel and antiparallel neighboring strands in the quadruplex. Three types of grooves exist in this structure: one narrow groove, two similar grooves of medium width, and one wide groove. Narrow and wide grooves are formed by antiparallel strands. Glycosidic bond conformations in the quadruplex stem alternate between syn and anti along the covalent linkage and are syn−syn−anti−anti in a quartet layer. All thymine residues in the loops are in anti. With the absence of high-resolution structural information about the location of ions in this structure, we decided to place three Na^+ cations into the channel. After equilibration, a 3.5-ns production simulation followed. From 0 to 2.0 ns, the rmsd value of the quadruplex stem fluctuated around 1.0 Å, indicating that the starting structure based on the NMR data was energetically relaxed. Subsequently, we noticed an increase in the rmsd value to 1.2 Å within 0.1 ns, remaining constant until 2.8 ns. The reason for this was found in a sudden slight mutual shift (displacement perpendicular to the helix axis) between the two guanine quartets located in the molecule center. Between 2.8 and 3.0 ns, the rmsd value increased to 1.6 Å, probably due to persisting deviations in the phosphate group positions, but then fell back to ca. 1.2 Å until the end of the simulation. Throughout the trajectory (Figure 6d), the glycosidic bond conformations were conserved. The closest interphosphate distances in the starting structure based on NMR data are 6.7, 8.6, and 16.1 Å across the narrow, medium, and wide grooves, respectively. The corresponding values averaged along the whole trajectory are similar, that is 7.4, 10.3, and 15.1 Å, respectively. We found more oscillations of various dihedral angles along the phosphodiester linkage in the central part of the structure compared to the previous simulations. Many angles typically changed in intervals of 50−500 ps; however, these changes did not reflect in any significant increase of the rmsd values of phosphate groups. A large part of these changes involving backbone dihedral angles occurred around 2 ns, coinciding with the aforementioned temporary displacement between the central two quartet layers.

It is instructive to compare the cross-channel O6−O6 distances. In the theoretical structure, the quartets are again symmetrical and the average O6−O6 distances are 4.3 Å for the outer and 4.2 Å for the inner quartets. In contrast, the outer quartets of the starting NMR structure are quite asymmetrical, with one O6−O6 distance at 3.9 Å and the other at 4.9 Å. The inner two quartets are almost symmetrical with O6−O6 distances of 4.3 and 4.1 Å.

Of the three cations we had placed into the central channel of the molecule, only one located between two terminal guanine quartet layers maintained its position throughout the simulation. Another cation placed between two guanine quartets at the opposite end of the quadruplex stem remained stable for 1.5 ns, but then rapidly moved out of the quadruplex stem, where it remained stacked close to the outermost guanine quartet layer. The cation moved back and forth between its original position within the quadruplex stem and this exposed position, where it was found between 1.5 and 1.8 ns, 2.0 and 2.6 ns, and around 2.9 ns for 70 ps. In the exposed position, this cation approached O2 keto groups of two thymine residues (first and third) in the diagonal loop forming coordinate bonds (O2−Na^+ distance 2.5 Å). Visual inspection shows that the loop sterically blocks the cation from moving further away from the channel entry (Figure 7b). The remaining cation that had been placed into the cavity in the molecule center stayed there for most of the time. However, at 2.1 ns, it briefly (for 250 ps) adopted a position within the cavity vacated by the cation displaced outside the stem (see above), staying close to the plane of the inner quartet layer of that cavity due to proximity of the outside cation kept in place by the loop. This movement correlates with the temporary dislocation between two central quartets described above.

The conformations of the two diagonal four-thymidine loops that exist in this structure do not deviate significantly from the initial experimental coordinates, having rmsd values around 1 Å along the trajectory. The first and fourth thymine residue of each loop are located on top of the outermost guanine quartet layers at either end of the quadruplex stem, where they stack on the imidazole rings of the aromatic guanine base heterocycles. These thymines are not coplanar and hydrogen bonds are not observed between them. During simulation, we observed the formation of single hydrogen bonds between thymine O2 oxygens and N3 hydrogen atoms of the first and third thymine residues in the loops, with a donor−acceptor distance of 2.8 Å and considerably buckled arrangements of the pairs.

Discussion

We have carried out altogether 25 ns of unconstrained MD simulations on both parallel and antiparallel quadruplexes

(34) Jing, N.; Gao, X.; Rando, R. F.; Hogan, M. E. *J. Biomol. Struct. Dyn.* **1997**, *15*, 573−585. Keniry, M. A.; Strahan, G. D.; Owen, E. A.; Shafer, R. H. *Eur. J. Biochem.* **1995**, *233*, 631−643.

(35) The rmsd's were calculated for structures averaged over the last 0.5 ns.

formed by oligonucleotides containing stretches of guanine residues that are arranged in stacked cyclically hydrogen bonded quartet layers. An interesting feature of these structures is the existence of a chain of monovalent ions carrying a positive charge in the center of these molecules. The focus of our investigation was the conformational flexibility and dynamic behavior of these guanine-rich DNA quadruplex molecules and, in particular, the role of the ions in stabilizing these structures.

Our simulations of the all-parallel d(G_4) quadruplex yield stable trajectories on a nanosecond scale, with exceptionally low fluctuations and close agreement between the experimental and theoretical structures with rmsd values of less than 1 Å. The base positions in these simulations remained largely constant, and the cyclically hydrogen bonded quartet layers are well-conserved. Highest deviations are found for the more flexible sugar phosphate backbone. This is consistent with experimental data derived from oligonucleotide crystal structure analyses. In fact, one phosphate group in the d(G_4) structure shifted its position during the simulation, adopting an alternative stable conformation, without affecting the attached sugar ribose ring. Actually, a similar mobility of individual phosphate groups was observed in oligonucleotide crystal structures solved at atomic resolution, where the coexistence (bistability) of two distinct conformations of individual phosphate groups in the crystal could be resolved.[4d,36] Furthermore, we have observed a similar behavior of an individual phosphate group previously in an unconstrained nanosecond MD simulation of a hemiprotonated four-stranded cytosine-rich i-DNA, d(C_4).[12] Our simulations also indicate that the parallel d(G_4) quadruplex structure is entirely stable with only two sodium ions in its channel.

The simulation without any ion in the channel of the molecule demonstrates the central role of cations for the stability of the guanine quadruplex. Drastic rearrangements occurred in the molecule, involving "walking" of one strand of the four-stranded molecule. Thus, the simulation temporarily produced a new "slipped" molecule with only three guanine quartet layers, an additional triad layer of guanine residues at one end of the quartet stem, and an isolated stacked guanine residue at the other pole. However, the slipped structure could be very efficiently stabilized by placing sodium ions back into the cavities between the guanine layers. In fact, upon adding the ions, the remaining three quartet layers very quickly recovered geometries virtually identical to the corresponding layers in the crystal structure. Only one of the four strands, the strand that had "slipped", showed an underwound conformation that significantly deviated from the crystal coordinates. This final structure was remarkably stable and showed in all aspects a behavior very similar to that of the original complete guanine quadruplex. Thus the lifetime of the "slipped" structure, once formed, is considerably above the nanosecond scale. In fact, temporary formation of guanine triads has been implicated in a proposed conversion pathway between alternatively folded guanine quadruplex conformers formed by telomeric DNA.[4i] On the basis of the experimental data we know that the native stem corresponds to the global minimum. On the other hand, the "slipped" structure can represent one of the intermediate metastable states during the last stages of G-stem formation. The transition between "slipped" and native stems can be induced by or correlated with an exchange of ions in the channel,[37] since when reducing the amount of cations in the channel both structures are destabilized and the barrier between them must be reduced. It is suggestive that the strand slippage could occur for instance when external force (stress) is applied on the stem along the quadruplex axis.

We have performed MD simulations of antiparallel guanine quadruplexes, namely of two conformational variants of a 1.5 repeat of the guanine-rich sequence found at the telomeres of *Oxytricha* chromosomes, d($G_4T_4G_4$). One set of simulations was based on the 2.3-Å resolution K^+-stabilized crystal structure of this sequence, while the other set utilized refined model coordinates based on nuclear magnetic resonance data recorded in the presence of Na^+ ions.[4a,b] The main difference between the crystal and NMR conformers is found in the geometry of the loops that are placed either across the edge of the guanine quadruplex (edge-looped, crystal) or across the diagonal of the guanine stem (diagonal-looped, NMR).

We carried out two simulations with either Na^+ or K^+ ions in the central channel of the molecule found in the crystal. Both simulations yielded a comparatively high rmsd value of the theoretical structures as compared to the crystal coordinates already after the initial equilibration period. In the further course of both Na^+ and K^+ simulations, however, the quadruplex stem remained entirely stable. Apparently, the crystal coordinates represent a comparatively high energy conformation of this molecule. This is also supported by the existence of quite close interphosphate contacts (3.9 Å) in the d($G_4T_4G_4$) crystal structure. We observed pronounced conformational flexibility of the four-thymidine edge loops in our simulations. This is in accordance with experimental data, which usually shows higher mobility for loop regions in molecules. In the crystal structure of d($G_4T_4G_4$), for instance, the isotropic temperature factors for the thymidine residues were elevated as compared to the guanine quadruplex stem, indicating that the loops were less constrained in the crystal, with the apical thymine residue being most flexible.[4a] The majority of changes of the loop geometries developed during equilibration and the very early stages of production simulation, including the formation of asymmetric T−T base pairs at the loop base. The trajectories seemed to be quite stable for the remainder of the simulations. However, the Na^+ and K^+ simulations utilizing the same starting geometry of the edge-looped structure resulted in two quite different nanosecond-scale stable conformations (substates) of one of the loops, with the Na^+ trajectory significantly deviating from the starting crystal data. We assume, that the difference in the cations is not the primary reason for the different behavior of that loop observed in the two simulations. Let us point out that this kind of MD simulation has a stochastic nature so that every simulation (trajectory) is unique. In contrast, the other loop present in this molecule remained close to its starting structure in both simulations. Its geometry, however, differs from both conformational substates obtained for the first loop since already in the crystal structure the two loops have different geometries. Thus we have obtained three different nanosecond-scale stable conformations of the edge loop. A proper interpretation of our results is that we do not have a complete sampling of the conformational space of the loops on nanosecond scale and that considerably longer simulation times would be required to achieve this.

The simulation of the NMR-derived conformer of d($G_4T_4G_4$) yielded a stable trajectory on a nanosecond scale, close to that of the experimental structure. One sodium several times temporarily escaped from the central ion channel and was then located at the stem loop junction between a terminal guanine quartet layer and a four-thymidine loop. The cation in this position is coordinated to O2 keto oxygen atoms of thymine

(36) Egli, M.; Williams, L. D.; Gao, Q.; Rich, A. *Biochemistry* **1991**, *30*, 11388−11402.

(37) (a) Xu, Q.; Deng, H.; Braunlin, W. H. *Biochemistry* **1993**, *32*, 13130−13137. (b) Hud, N. V.; Schultze, P.; Sklenář, V.; Feigon, J. *J. Mol. Biol.* **1999**, *8*, 233−243.

residues in the loop. One can imagine that, due to direct cation-loop interactions of the kind described, cations could influence the equilibrium of formation between for instance edge-looped conformers (as found in the crystal) and diagonal-looped conformers (derived from NMR data) of $d(G_4T_4G_4)$ or other looped guanine quadruplex structures. It has to be emphasized that the time scale of a complete ion exchange is hundreds of microseconds to hundreds of milliseconds,[37] that is several orders of magnitude above the time scale of current computer experiments. On the other hand, the MD simulations definitely allow at least some insight of the cation mobility at the atomic level. Our rather short simulation obviously does not allow us to investigate a complete exchange of the cation between the channel and the solvent.

Let us now assess the reliability and limitations of the theory used. Properties of G-DNA quadruplex stem structures are significantly influenced by stacking and hydrogen bonding of DNA bases. As demonstrated elsewhere,[10] the Cornell et al. force field provides a fairly good description of stacking and hydrogen bonding of bases. More difficulties were reported concerning the way current empirical potentials approximate the conformational flexibility of the sugar−phosphate backbone.[11i,q] This explains differences in sugar puckering in the theoretical structure compared to the atomic resolution crystal coordinates. Nevertheless, due to the unusual rigidity of G-DNA quadruplex stems, the molecule is efficiently locked in the optimal structure. Thus, overall consequences of inaccuracies in the backbone parametrization should be small, at least compared for example to simulations of the interconversion between B-form and A-form DNA.[11b,f,i] We expect that the behavior of loops will definitely be more sensitive to the force field.

Apparently the largest inaccuracy in the force field description occurs for the direct (short range) interaction between the G-layers and cations. Cation-containing complexes of nucleic acid bases show pronounced polarization effects, and the electronic structure of the cations and ligands is important.[28,38] These effects are neglected by the pairwise additive force field, and we believe that it influences several aspects of our simulations. First, in contrast to crystal data, the Na^+ cations in our simulations did not occupy a position in-plane of a guanine quartet layer hinting at possible overestimation of the radius of the cation in the evaluation of the guanine−cation contact. This has been confirmed in this study by ab initio calculation. Reduction of the radius of the "force field" cation improves the mobility of cations in the structure. However, it does not eliminate the other artifact observed, namely, a bifurcated type of hydrogen bonding of the inner quartets. This indicates some deeper problems in the description of the interactions which cannot be repaired by adjusting the Lennard-Jones parameters. Actually, an ab-initio-optimized structure of an isolated G-quartet with a Na^+ cation shows correct hydrogen bonding without bifurcation.[39] Also, the calculations did not show significant differences for a guanine quadruplex stem simulated with K^+ or Na^+, respectively. This finding does not appear to agree with NMR data,[5d] suggesting a weaker pairing in the quartets for larger K^+ ions. It is likely that the experimentally observed differences between the Na^+- or K^+-stabilized structures are partly due to specific electronic effects which are not included in the current force field. We emphasize that the uncertainty of the empirical potential description of direct interactions between a cation and guanine quartet layers should not introduce any significant error into the overall outcome of simulations since the leading long-range electrostatic term is properly included.

Formation of G-DNA structures in experiments takes from hours to days. Thus we should not expect that nanosecond-length simulations are able to disclose all aspects of the dynamics and folding of these structures. For example, the calculations show that both a cation-stabilized G-stem with four intact guanine quartet layers and the cation-stabilized G-stem with a "slipped" strand with three quartets and one triad represent stable conformations of parallel $d(G)_4$. However, we could not evaluate their relative stability since we did not see any interconversion between them in the presence of cations in the channel. Similarly, when simulating the intermediate "spiral" G-DNA structure without cations in the channel, we have seen that strand D behaves differently from the others throughout the whole simulation, even though all strands should be equivalent on a long time scale, due to the inherent 4-fold symmetry of the parallel $d(G)_4$ quadruplex. One important example of the limitations imposed by the simulation length is the behavior of the four- thymidine edge loops discussed in detail above. Much longer time scales would be necessary to guarantee a complete sampling of the conformational space of the loops.

Let us now compare our study with preceding theoretical studies on G-DNA. A careful examination of the base stacking energy of various possible arrangements of consecutive G-quartets was reported by Strahan et al.,[5f] in order to illuminate whether the base stacking difference could rationalize the absence of anti−syn stacks in the experiment. The energy evaluation was carried out utilizing the Weiner et al. force field[40] (old AMBER force field), and the solvent effects were approximated using a distance-dependent dielectric constant. The stacking geometries were obtained via in vacuo MD simulations. The van der Waals component of the base stacking energy was found to be in the range −43 to −49 kcal/mol, in good agreement with the values presented here. The electrostatic energy was found to be negligible due to the use of the distance-dependent dielectric contrast. In contrast to our study, Strahan et al. did not report the quartet−cation stacking energy while we believe that it is an integral component of the stacking. A very important result of the calculations by Strahan et al. is that all studied quartet stacks are essentially equally stable (within the range of 4 kcal/mol) with the anti−syn stack being least stable. Therefore, they suggest that base stacking could contribute to the absence of the anti−syn arrangement in the experiment. One could however note that the 4 kcal/mol difference is exceptionally small.

Bansal and co-workers carried out a set of in vacuo molecular mechanical model building studies supplemented by limited in vacuo MD simulations[5b,e,g] considering a number of folding topologies of various G-DNA molecules including structures with nonguanine quartets. Direct comparison of our results with the Bansal et al. study is not straightforward since the studies address different problems. Our simulations were not designed to compare stabilities of various folding patterns. On the other hand, the presently used model of G-DNA with explicit inclusion of solvent and cations, using an improved force field and based on nanosecond-scale MD simulations, represents a very considerable advance in the reliability of theoretical descriptions of nucleic acids.[11e,h,n] Similar to our results, Bansal and co-workers predict the formation of T−T pairing in loop

(38) Šponer, J.; Burda, J. V.; Mejzlík, P.; Leszczynski, J.; Hobza, P. *J. Biomol. Struct. Dyn*. 1997, *14*, 613−628.

(39) Gu, J.; Leszczynski, J. Manuscript in preparation.

(40) Weiner, S. J.; Kollman, P. A.; Case, D.; Singh, U. C.; Ghio, C.; Alagona, G.; Profeta, D. S., Jr.; Weiner, P. J. *J. Am. Chem. Soc*. **1984**, *106*, 765−784.

regions of telomeric DNA. Here, all currently available theoretical studies are in complete agreement.

An extensive computational analysis of ion-induced stabilization of the G-DNA molecules based on MD and free energy perturbation studies was published by Ross and Hardin.[5a] They concluded that the calculations are not capable of explaining the observed Na^+/K^+ selectivity, and they attributed this to the deficiency of the simple pair-additive force field to account for electronic effects not captured by the electrostatic model (polarization and charge transfer). We came to the same conclusion on the basis of the evaluation of the mobility of the cations in the channel, artifacts in the base pairing, and quantum-mechanical calculations. Similar to other theoretical studies, Ross and Hardin noticed the formation of thymine self-base pairs, in their particular case of interloop hydrogen bonds for a $d(T_2G_4)_4$ antiparallel structure. A striking difference between our study and that by Ross and Hardin is the pronounced instability of their structure with three cations in the channel (see description on p 6073[5a]). This can be easily explained since Ross and Hardin did not use the PME method; this method was not available at that time. Without using the PME protocol, all hydrated DNA simulations are necessarily unstable due to improper treatment of the electrostatics and this instability must be especially large for G-DNA with the closely spaced cations in the channel. Thus, all instabilities observed by Ross and Hardin are due to the treatment of long-range electrostatics inherent to all older (non-PME) MD studies on hydrated oligonucleotides.[11e,h,n]

The study which is most closely related to our contribution is the NMR analysis of a $d(G_3T_4G_3)$ hairpin dimer structure performed by Strahan et al.[5d] The authors used short PME MD simulations as an integral part of their refinement protocol. Their simulations started with 0.25−0.3 ns of restrained MD simulation (using restraints derived from NMR data) followed by 0.45−0.5 ns of unrestrained simulations. Two K^+ cations were placed in the two cavities of their G-stem. They were able to demonstrate that the inclusion of the PME technique improves the refinement protocol. In agreement with our data, they observed hydration of the grooves, formation of hydrogen bonds in the loops, and a certain plasticity of the loop structure, supported also by the NMR data indicating two conformations. A direct comparison with our study however is not simple as they studied a different molecule in the presence of K^+, while we mostly used Na^+. In addition, their unrestrained simulations were actually quite short. Interestingly, they observed a pronounced asymmetry of the central G-quartet in the course of restrained simulations while this quartet became symmetrical during unrestrained simulation. We have observed a similar behavior of the outer quartets in the simulation of the diagonally looped $d(G_4T_4G_4)$ NMR conformer.

Finally, let us mention recent studies that do not have G-DNA to their theme but present developments of new techniques that might be useful in theoretical studies of G-DNA soon. The locally enhanced sampling technique (LES) might help to lower the actual energy barriers among various substates of the loop regions and allow faster relaxation toward optimal structures.[11m] Supplementing the MD simulations by calculations based on continuous treatment of electrostatics could allow at least a crude estimate of the free energy difference between various substates where there is no interconversion during the simulation (it might in our case allow estimation of the free energy difference between the native and "slipped" G-stems).[11k,l] It still remains to be seen how robust these methods are. However, in all cases, the large-scale PME MD simulations as presented here will constitute the major part of the modeling.

DNA is a polymorphous molecule and can adopt a variety of molecular conformations. Examples for unusual DNA architecture are four-stranded assemblies such as the guanine quadruplex that is the focus of this contribution. The guanine quadruplex itself is capable of adopting a variety of conformers, such as the all-parallel quadruplex or antiparallel quadruplex molecules formed by sequences such as $d(G_4T_4G_4)$. Even one particular sequence, $d(G_4T_4G_4)$, can adopt at least two different conformations, with loops on the edges or across the diagonal of the guanine quadruplex stem. Cations lining up in the ion channel form an integral part of these sophisticated molecules. In fact, it appears that the choice of ions plays a central part in the interconversion of the different conformers of a guanine rich sequence, as exemplified by the observation of a sodium−potassium switch in the formation of guanine quadruplex DNA.[41]

In the genome of cells, for example in telomeres, sequences containing stretches of guanine residues (apart from the short 3′ terminal overhangs) are paired to a strand containing stretches of cytosine residues. It is interesting to note that both guanine-rich and cytosine-rich sequences including telomeric DNA motifs are capable of adopting stable four-stranded structures, albeit entirely different in their architecture. Both DNA quadruplex motifs have in common a spine of positive charges lining up along the helical axis in the center of the molecules. In the case of the guanine quadruplex, this spine is formed by monovalent cations that occupy the cavities between adjacent guanine quartets, involving coordinate bonds to the guanine O6 oxygen atoms. The cations in these structures are separated by approximately 3.4 Å in accordance with the spacing between the quartet layers where overt stacking of the aromatic base heterocycles occur. In the case of four-stranded intercalated cytosine-rich DNA, in contrast, the consecutive positive charges in the molecule center stem from the hemiprotonation of the $C{\cdot}C^+$ self-base pairs. In this structure the adjacent $C{\cdot}C^+$ base pairs are more closely spaced (3.1 Å). We have determined the net energy of the vertical interactions in the guanine quadruplex (this contribution) and previously also in four-stranded intercalated cytosine-rich i-DNA.[12,14] We found that the vertical interactions in the guanine quadruplex were always stabilizing, while in i-DNA, the contribution is quite repulsive. Notwithstanding, both structures show similar behavior in simulations and are exceptionally stable on the nanosecond scale, clearly underscoring the unusual conformational rigidity of these four-stranded molecular assemblies. We believe that the rigidity of G-DNA and i-DNA quadruplexes could constitute a rather unique mechanical property of these molecules. This could be important for instance for the molecular recognition of these motifs by specific proteins.[41] Guanine- and cytosine-rich sequences can clearly form compact and rigid DNA segments, possibly capable of spacing or localizing other more flexible parts of the DNA in the nucleus of cells.[4a,13d] In addition, they can be used as versatile molecular building blocks for novel, nucleic acid based synthetic catalysts for a variety of functions in chemistry, diagnostics, and therapy.[42,43] Theoretical approaches as presented in this contribution, complementing high-

(41) Sen, D.; Gilbert, W. *Nature* 1990, *344*, 364−366.

(42) (a) Weisman-Schomer, P.; Fry, M. *J. Biol. Chem.* **1993**, *268*, 3306−3312. (b) Fang, G.; Cech, T. R. *Cell* **1993**, *74*, 875−885. (c) Liu, Z.; Frantz, J. D.; Gilbert, W.; Tye, B.-K. *Proc. Natl. Acad. Sci. U.S.A.* **1993**, *90*, 3157−3161. (d) Schierer, T.; Henderson, E. *Biochemistry* **1994**, *33*, 2240−2246.

(43) (a) Ellington, A. D. *Curr. Biol.* **1994**, *4*, 427−429. (b) Gold, L.; Polisky, B., Uhlenbeck, O.; Yarus, M. *Annu. Rev. Biochem.* **1995**, *64*, 763−797. (c) Stull, R. A.; Szoka, F. C., Jr. *Pharm. Res.* **1995**, *12*, 465−483.

resolution structural studies, will be instrumental for properly understanding the actual sources of stability of these unusual molecular conformations that DNA can adopt.

Conclusions

The G-DNA quadruplex stems are exceptionally rigid molecules and should have unique mechanical properties that contrast those of most other nucleic acid forms. Interestingly, one other four-stranded motif, i-DNA, exhibits the same rigidity. A rather striking difference between G-DNA and i-DNA is that G-DNA has an attractive net vertical (stacking) interaction along the helix axis, since the cation−cation repulsion is compensated for by the stacking interactions involving the extended guanine quartets.

G-DNA stems can adopt an alternative conformational substate with a slipped strand. This conformational substate shows close to identical stability and dynamical behavior as the native G-stem on the nanosecond time scale.

The monovalent cations in the channel of the G-DNA stems represent an integral part of these structures. The G-DNA stems can sustain a certain reduction of the number of cations in the channel without any significant perturbation. Thus an exchange of cations with the solvent is possible without causing any deformation of the stem. However, complete removal of the cations from the channel leads to immediate (picosecond-scale) destabilization of the structure. A stable or nondeformed structure of a quadruplex molecule is not possible without a significant occupancy of the channel by monovalent cations. The simulations further show the cavities being hydrated on a scale of 100 ps or less when being left vacant by a cation, but the hydration itself is not sufficient to stabilize the structure.

In antiparallel G-DNA hairpin structures studied here, the thymines of diagonally placed loops are capable to temporarily coordinate (recognize) cations residing in the channel while similar interactions are not present in the edge-looped structures. Formation of stable interthymidine hydrogen bonds in the loops is observed wherever possible, and this trend is apparently more pronounced for the edge looped than for the diagonal looped molecules.

The simulations consistently show that the G-quartets are symmetrical (as measured by diagonal O6−O6 distances), independent of the structure simulated (parallel or antiparallel, diagonal looped or edge looped, K^+ or Na^+ stabilized). Even if the simulations start with asymmetrical quartets, symmetry in the layers is immediately achieved. This result is consistent with the high-resolution crystal structure of parallel-stranded G-DNA. However, asymmetrical quartets are rather frequently reported in NMR studies. The reason for this discrepancy is not clear, but we are not aware of any defect of the force field which could rationalize the symmetry of all quartets as a simulation artifact.

When applying the PME method, the simulations properly include the dominating electrostatic part of the cation−solute interactions and provide a very realistic picture of the molecular dynamics. However, due to the pair additive nature of the potential used, short-range polarization effects are neglected. To our best knowledge this is the first PME MD study to address this issue, identifying artifacts that are likely associated with the deficiency of the force field even for monovalent alkaline metal cations. The most important deficiencies are a restricted mobility of the cations in the channel and the appearance of a bifurcated hydrogen bonding pattern in the inner quartets of G-stems stabilized by Na^+, which is not in agreement with the atomic resolution experiment. Our assumption, that force field inaccuracies due to a neglect of polarization effects constitute the likely physical origin of these artifacts, is further supported by ab initio quantum chemical calculations for cation−base interactions reported here and elsewhere. Probably, the accuracy of the currently available nonpolarizable force fields is not sufficient for addressing subtle issues such as specificity of Na^+ and K^+ cations, advising for caution in any respective attempts.

An additional limitation imposed is the nanosecond scale of the simulations, which is not sufficient for providing a complete sampling of the thymidine loop regions of antiparallel hairpin structures. The edge loop regions appear to exist in several substates separated by considerably high energy barriers and with lifetimes that are well above the nanosecond scale. Thus, important substates might not be detected even when making very long unrestrained simulations.

Acknowledgment. This study was supported by the Grant A4040903 by IGA AS CR and by the Grant 203/97/0029 by GA CR. I.B. is supported by a Liebig fellowship from the Fonds der Chemischen Industrie (FCI, Germany). All calculations were carried out in the Brno Supercomputer Center and Prague Supercomputer Center. We thank the (anonymous) reviewers for a very careful reading of the manuscript and a number of valuable comments. J.Š. thanks Dr. M. Orozco for a helpful discussion.

JA984449S